# ELECTROCHEMICAL AND MICROBIAL TREATMENT OF BROMOPHENOL BLUE (BB) AND MALACHITE GREEN (MG) DYE CONTAMINATED WATER FOR ELECTRICITY GENERATION

**BY**

**ANYANWU, JOHN OJINERE**

**(B.Tech, Industrial Chemistry)**

**ACEFUELS/20/MSc/13000121**

**A THESIS SUBMITTED TO THE AFRICA CENTER OF EXCELLENCE IN FUTURE ENERGIES AND ELECTROCHEMICAL SYSTEMS (ACE-FUELS), FEDERAL UNIVERSITY OF TECHNOLOGY, OWERRI (FUTO)**

**IN PARTIAL FULFILMENT OF THE REQUIREMENTS FOR THE AWARD OF THE DEGREE OF MASTER OF SCIENCE (M.Sc.) IN FUTURE ENERGIES**

**AUGUST, 2023**

## CERTIFICATION

This is to certify that this research was carried out and written by me, John Ojinere Anyanwu, (Reg. No: ACEFUELS/20/MSc/13000121) a Master's Degree Student of Future Energies programme at the Africa Centre of Excellence in Future Energies and Electrochemical Systems (ACE-FUELS), Federal University of Technology, Owerri (FUTO).

.....
Prof. T.E. Ogbulie
(Supervisor)

Date 24/08/2023

.....
Dr. K.L. Oguzie
(Co-supervisor)

Date 24/08/2023

.....
Prof. A. I. Opara
(Programme Coordinator
Future Energies)

Date 24/08/2023

.....
Prof. E. E. Oguzie
(Centre Leader, ACE-FUELS)

Date 14/9/23

.....
Prof. B. O. Esonu
(Dean, PGS)

Date .....

.....
Prof. P. C. Okafor
(External Examiner)

Date 10 August, 2023

# DEDICATION

This paper is dedicated to my institution's mentors, without whom I could not have completed this thesis. They not only provided me with academic knowledge, but they also provided me with valuable advice when I needed it the most.

# ACKNOWLEDGEMENTS

This work was carried out at the ACE-FUELS laboratory domiciled in the Federal University of Technology, Owerri. This study was done under direct supervision of Prof.T.E Ogbulie (Department of Biotechnology, FUTO), Dr.C.O.Akalezi (Department of Chemistry, FUTO) and Dr. K.L Oguzie (Department of Environmental Science, FUTO).

First and foremost, I will like to show my deepest appreciation to my team of supervisors. I want to express my heartiest gratitude to Prof.T.E Ogbulie for her innovative ideas and guidance on microbial trearment of wastewater . Special thanks also to her other students (Miss Mberede and Mrs Chidinmma) for their assistance and direction during the isolation, identification and culturing of the micro-organisms. Special thanks to Dr. K.L Oguzie for her invaluable insights, skills and guidance during the electrochemical treatment method. Also I will like to express my sincere gratitude to Dr.C.O Akalezi for his assistance on kinetic approach of this study and also for painstakingly proof-reading my thesis. Without their assistance and dedicated involvement in every step throughout the process, this paper would have never been accomplished.

My sincere thanks to Prof E. E Oguzie who doubles as the Center Leader of ACE-FUELS and DVC Research and Innovation, FUTO whose excellent leadership ability has propelled the center to an enviable status. Special thanks to him also for making sure that all instrument required for this study were quickly for as when requested and also many thanks to him for his genius guidance on the microbial fuel cell experiment.

I would like to express my deepest appreciation to the Africa center of excellence in future energies and electrochemical systems (ACE-FUELS) for the partial scholarship and research grant awarded to me, without which I could not have undertaken this journey.

Special thanks to Dr.Simeon Nwanonenyi for his guidance on the use of material studio. I am also grateful to the entire ACE-FUELS staff and students for their unrelenting support throughout the

programme. . I would like to thank you very much for your support and understanding over these past one year.

Lastly, I would be remiss in not mentioning my family, especially my parents and siblings. Their belief in me has kept my spirits and motivation high during this process.

TABLE OF CONTENTS

# LIST OF TABLES

# LIST OF FIGURES

# ABSTRACT

Pollutants present in textile waste water are recalcitrant and difficult to treat with simple processes. In this study, an energy-sustainable method for treating dye-contaminated water was devised by combining an electrochemical process and a microbial fuel cell. An electrochemical oxidation procedure using copper cathode and graphite anode electrodes was employed for decolorizing Malachite green (MG) and Bromophenol Blue (BB) dye in an aqueous solution. Bio-electricity was generated using BB and MG dye-contaminated water in a dual chamber MFC. Micro-organisms isolated and cultured from MG and BB dye-contaminated soil were also employed to determine their efficiency in degrading dye-contaminated water. The isolated micro-organisms were identified as *Eubacterium sp* (M2*)*, *Streptobacillus sp* (M3), *Aspergillus niger* (B6), *Trichophyton terrestre* (M4*) Serratia marcescens* (B2), *Acinetobacter baumanni* (B1), *Bacillus subtilis* (B3*), Bacillus megaterium* (B5), *Aspergillus Flavus* (B7), *Rhizopus stolonifer* (B8) respectively. Decolorizing ability of dyes was observed by dye decolorization assay. *Streptobacillus sp* achieved the highest degradation efficiency of 95.6 % for MG while *Serratia marcescens* achieved the highest degradation efficiency of 45.3% for BB. The impacts of a number of variables, including the supporting electrolyte, temperature, current density, and pH on the electrochemical dye removal process were investigated. While decolorization effectiveness exhibited a nonlinear pattern with pH and temperature, it increased gradually with current density and electrolyte content. With 100% maximum effectiveness, obtained at pH 3 for BB and 98.5% obtained at pH 5 for MG, while maximum efficiency of 98.3% was obtained at $38^0$C for both MG and BB. The maximum OCV and power density achieved by MG based MFC is 0.7 2V and 8.33 mW/m$^2$ while the maximum OCV and power density for BB based MFC is 1.28 V and 167.45 mW/m$^2$. Density functional theory-based quantum chemical computations indicate oxidative attack to be initiated at the Bromine atom of the hydro-phenyl group for BB and at Carbon atom of the methylene group for MG.



**Keywords: Microbial fuel cell, Decolorization, Microbial degradation, Fukui indices, Electrochemical, Density Functional theory.**

# CHAPTER ONE

# INTRODUCTION

## 1.1 Background Information

Our world is reaching new heights as a result of the growth of mankind, society, science, and technology, but the price we are paying or will pay soon is too great. One of the results of this fast expansion is a major environmental disaster. Water pollution occurs when dangerous substances, most typically chemicals or microbes, pollute a stream, river, lake, ocean, aquifer, or other body of water, lowering water quality and making it poisonous to humans or the environment. Agricultural, industrial, and domestic sectors consume 70%, 22%, and 8% of available fresh water, respectively, resulting in the generation of large amounts of wastewater containing many 'pollutants'(Gupta, 2009; Makarem, 2018). Aromatic amines, which are intermediate components of azo dyes, may be carcinogenic in humans. Dyeing wastewater pollution has been a big issue in the developing world, and scientists are working to reduce pollution by inventing new materials and methods.

### 1.1.1 Pollutant

A pollutant is a substance or energy introduced into the environment that has undesired effects, or adversely affects the usefulness of a resource. Pollutants can cause long-term or short-term harm. Pollutants, an omnipresent and concerning aspect of our modern world, are substances or agents that infiltrate our environment and pose a significant threat to the delicate balance of nature. These harmful elements can arise from both natural processes and human activities, tainting the air we breathe, contaminating the water we rely on, and degrading the soil that sustains life. From toxic industrial emissions to everyday household waste, pollutants have far-reaching implications, impacting both human health and the well-being of ecosystems. Understanding, monitoring, and addressing pollutants are vital endeavors if we are to safeguard the planet's health and secure a sustainable future for generations to come. Dye pollution is an important category of contaminants, and once it gets into the water, it may be challenging to remove and remediate.This is due to the dyes' synthetic origin and complex molecular structure, which makes them more stable and difficult to biodegrade (Bhattacharyya & Sarma, 2003; Forgacs *et al*., 2004). Dye molecules can withstand degradation even when subjected to high temperatures, oxidizing agents, or bright light

(Crini, 2006; Forgacs *et al*., 2004; Peng *et al*., 2018). Textiles and non-textile applications of dyes include liquid crystals, acid-base indicators,biomedical, color filters for displays, ink-jet lasers, sensors, etc (Sabnis, 2017).

### 1.1.2 Types of Dye

Dyes have a wide range of structural characteristics and are classified in a variety of ways. Dyes are sometimes classified based on their application and structure. Azo dye, Nitro dye, Phthalein dye, Triphenyl methane dye, Indigoid dye and Anthraquinone dye are classified on the basis of their structure. Whereas, Acid dye, Basic dye, Direct dye, Ingrain dye, Disperse dye, Moderate dye, Vat dye and Reactive dyes are classified on the base of their application

**Malachite Green**

Malachite green is a triphenylmethane dye that is used to color silk, wool, jute, and leather as well as cotton that has been mordant with tannin. Malachite green has antifungal and antibacterial properties. It has been employed in the fish breeding business to suppress the fungus *Saprolegnia*, a water mold that destroys the eggs and young fry. The dye, which is made from benzaldehyde and dimethylaniline, appears as shiny green crystals that are soluble in water and alcohol.

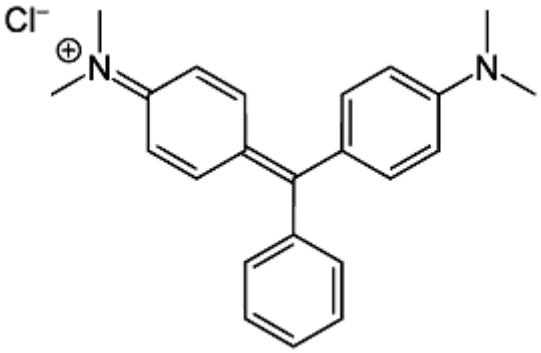


**Figure 0.1 The chemical structure of Malachite Green**

**Bromophenol Blue**

Bromophenol blue (BB), a significant triphenylmethane derivative, is frequently used as a laboratory indicator and organisimal stain in sectors such as silk, leather, medicines, and copy. Bromophenol blue is also used as a dye. At neutral pH, the dye absorbs red light most strongly and

transmits blue light. (Its peak absorbance is 590 nm at a basic pH of 12). As a result, the dye's solutions are blue. The dye looks yellow in solution when the pH is low because it absorbs UV and blue light the most effectively. Bromophenol blue has a distinctive green red color in solution at pH 3.6 (in the middle of this pH indicator's transition range) obtained by dissolving in water without any pH adjustment. The apparent color changes depending on the concentration and/or path length through which the solution is observed. It is known as dichromatic color for this behavior. It used as acid-based indicator, color marker and dye.

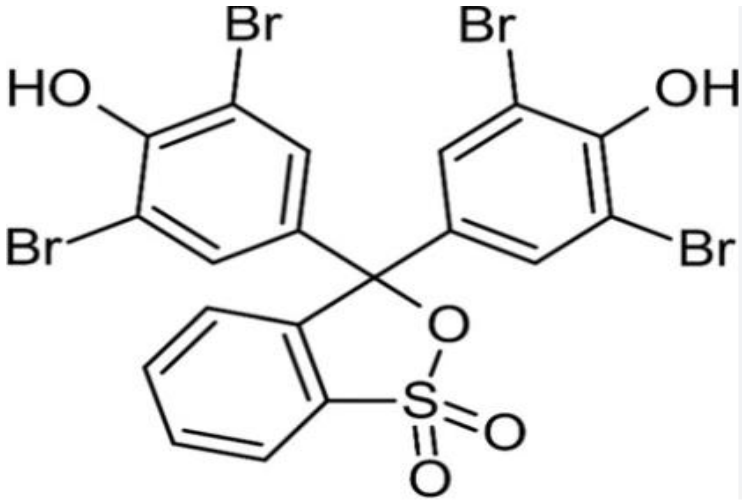


**Figure 0.2 The chemical Structure of Bromophenol blue**

### 1.1.3 Effect of Water Pollution on Man and His Environment

One of the most serious consequences is disease. According to the World Health Organization, cholera kills over 120,000 people each year. Furthermore, the Fukushima disaster increased the risk of thyroid cancer in newborns by 70%. The introduction or removal of specific microbes alters the ecosystem. Nutrient pollution, for example, causes algae to grow, depleting the oxygen in the water and killing fish and other aquatic life.

### 1.1.4 Water Pollution Treatment Method

Wastewater treatment is a process used to remove contaminants from wastewater and convert it into an effluent that can be returned to the water cycle. Processes commonly used in wastewater treatment include

- **Electro-oxidation (EO)**;

  Electrochemical oxidation also known as anodic oxidation is a type of advanced oxidation process used for wastewater treatment, primarily for industrial effluent. The most basic configuration consists of two electrodes, an anode, and a cathode, connected to a power source. When the system receives an energy input and a sufficient supporting electrolyte, strong oxidizing species form and interacts with the contaminants, degrading them.

- **Microbial Method;**
  Microbial Wastewater Treatment is concerned with the use of microorganisms as a decontaminating tool in the treatment of polluted wastewater. Microbial decoloration can occur through two main mechanisms: biosorption, enzymatic degradation, or a combination of the two.

- **Microbial fuel Cell (MFC);**
  A microbial fuel cell (MFC) is a device that uses microorganisms to transform chemical energy into electrical energy. A bioanode and/or a biocathode are used in these electrochemical cells. There are two types of MFCs: mediated and unmediated. It is used in biosensors, power generation, and wastewater treatment.

## 1.2 Problem Statement

Every year, estimated $70x10^6$ tons of synthetic dyes are produced and primarily used in the textile, cosmetics, leather, and other industries, with 30-150 thousand tons of dye effluent discharged into bodies of water. These dyes pollute the sediment, soil, ground water and surface water systems, thus providing a significant problem for global pollution. Due to the massive amounts of water that need to be cleaned as well as the visible high levels of toxins present, conventional wastewater treatment is an expensive and energy-intensive procedure.

## 1.3 Aim and Objectives

The aim of the study is to investigate the treatment of dye-contaminated water and the simultaneous generation of electricity using coupled electrochemical and microbial methods

The objectives of this study are:

1. Isolation and identification of micro-organisms that can degrade malachite green and bromophenol blue dye.
2. Determination of the efficiency of the microbial degradation of malachite green and bromophenol blue contaminated water.
3. Determination of the efficiency of the electrochemical degradation of malachite green and bromophenol blue dye contaminated water.
4. Generation of bio-electricity from a microbial fuel cell.

## 1.4 Justification of Study

Electrochemical processes consume a lot of energy (Mohanakrishna *et al.*, 2021) while microbial fuel cells that use bacteria as a bio-catalyst are known to effectively treat waste water with no energy input (Kumar *et al*., 2019; Malyan *et al*., 2019). Due to its robust advantages such as ease of use, electrochemical system waste water treatment is one of the most commonly used treatment methods, and it has been proven to be a far better stand-alone technique than other physicochemical methods. The efficiency of microbial fuel in wastewater treatment and electricity generation is well documented.

## 1.5 Scope of Study

Three different experiments were performed:

**Microbial degradation studies**

- Dye: Mineral salt
- Duration: 9 weeks

**Electrochemical studies**

- Temperature ($28^0$C, $38^0$C, $48^0$C, $58^0$C)
- Current density (0.27, 0.53, 0.8, 1.07, 1.33 mA/mm$^2$)
- Electrolyte concentration (1, 0.5, 0.1, 0.05 M)

- pH (3, 5, 7, 9, 11)

**Microbial Fuel Cell**

- Electrode material (Carbon felt, Graphite plate),
- Open circuit voltage
- Resistance (330,100 ohms)

# CHAPTER TWO

# LITERATURE REVIEW

Dye effluents are now a major source of environmental concern in wastewater treatment. Textile industries consume a large amount of water and generate a significant amount of wastewater, which contains unconsumed dyes and constituents, posing a serious problem for wastewater treatment plants. Textile effluents contain high levels of color, TDS, and toxic metals, which have been linked to a decrease in the capacity of pollutants in wastewater to degrade themselves. This review of the literature supports the claim that stand-alone dye waste water treatment methods are not very inefficient at degrading dye and producing electricity, but a combination of methods will. Literature on the microbial method, electrochemical method, microbial fuel cell, and the combined process was reviewed.

## 2.1 Dye as a Pollutant

When dyes have completed their duty in coloring materials, dye-using companies often store dye effluents as industrial waste (Solís *et al.*, 2012). An estimated 100,000 commercially available dyes are used to produce 700,000 tonnes of different colorants each year. ( Gupta *et al*., 2009; Abdi *et al.*, 2017; Crini, 2006; Katheresan *et al*., 2018). The bulk of dyes are carelessly dumped into environmental water bodies once they have served their purpose. Color, PH, suspended particles, COD, BOD (Yaseen & Scholz, 2017), metals (Sekomo *et al*., 2012; Sharma *et al*., 2007), and salts are all high in dye effluents.

These pollutants are subsequently disposed of in the environment's water bodies, converting colorless pure water into tainted colored water. The presence of dyes in water is undesirable to environmentalists and the general public since they are harmful poisonous compounds (Masindi & Muedi, 2018). Dyes are regarded as an unpleasant form of pollutant since they are hazardous (Bae & Freeman, 2007), mostly by oral consumption and inhalation, skin and eye irritation, and skin sensitization, resulting in issues such as skin irritation and skin sensitization, as well as carcinogenicity (Banerjee, 2007; Christie, 2007). They alter the color of the water, which is visible to the naked eye and hence quite unappealing. Not only that, but they also interfere with light

transmission and disrupt biological metabolic processes, destroying aquatic communities in the environment ( Rafatullah *et al*., 2010; Maleki *et al.*, 2017; Zeng *et al.*, 2017).

Dyes also have a tendency to sequester metal, which might cause microtoxicity in fish and other animals. Therefore, it is essential to remove dye from colored effluents. The majority of dye effluents discovered in the environment globally (more than half) are produced by the textile industry (54%) and account for more than half of all dye effluents. Significant amounts of dye effluent are produced by the dyeing sector (21%) as well as the paper and pulp (10%), tannery and paint (8%), and dye manufacturing (7%) industries, all of which are related activities. (De Gisi *et al.,* 2016; Mojsov *et al.*, 2016). Although the precise quantity of dye effluents released into the environment by each industry is unknown, it is high enough to pose a significant threat to the ecosystem. The textile sector is said to utilize more dyes than any other industry, consuming more than 10,000 tonnes annually on a global scale (Rodríguez-Couto *et al.*, 2009).

Furthermore, this company is reported to create around 100 tonnes of dye effluent per year, the biggest volume of dye wastewater from a single industry (Solís *et al*., 2012). Furthermore, textile manufacturers generate large volumes of dye effluent due to the industry's high water demand ( Chacko & Subramaniam, 2011; Salleh *et al.*, 2011; Adegoke & Bello, 2015). Specific chemical, dyestuff, and water mixes are created for various processes in the textile business. When the procedure is finished, the remaining mixture (dye effluent) is released into the environment. For example, 85% of dye effluent from the dyeing process is expelled. Dye effluents from the textile industry are thought to exist because the dye combination (dye molecules and chemicals) is unable to completely attach itself to fabric or cloth. Due to their restricted absorption capacity, fabrics, for instance, can only absorb a maximum of 25 % of the dye mixture onto their body. One of the most challenging industrial wastewater to treat is dye wastewater from the textile and dyestuff industries (Nguyen & Juang, 2013). Dyes are resilient and difficult to biodegrade due to their synthetic origin and complex aromatic compounds (Ali, 2010). Currently, several research publications claiming successful dye removal have established various dye removal procedures.

**a2.2 Microbial Treatment Method**

Bacterial treatment is a less expensive and more environmentally friendly option for color removal in textile effluents. The ability of microbes to degrade synthetic dyes has been linked to enzyme production during degradation. Chen *et al*.(2008) investigated *Shewanella Sp.* biodegradation of crystal violet. They isolated the bacterial isolate, strain NTOU1, from an oil refinery's cooling system and used morphology characters, gyrase subunit beta gene, the 16S rRNA gene, biochemical test and gram staining to identify the strain as a member of *Shewanella decolorationis* (gyrB). The scientists found that this strain needed a pH of 8 to 9 and a temperature of 30 to 40 °C in order to decolorize crystal violet under anaerobic circumstances. They discovered that Formate (20 mM) was the best electron donor and that the addition of ferric citrate did not inhibit crystal violet decolorization, that the addition of thiosulfate, ferric oxide, or manganese oxide slightly decreased decolorization, and that the addition of nitrite (20 mM) inhibited crystal violet decolorization. However, by supplementing the medium with formate and ferric citrate and cultivating it at optimal pH and temperature, the strain was able to remove crystal violet at a concentration of 1500 mg/L at a rate of 298 mg $L^{-1}$ $h^{-1}$ (the $OD_{600}$ of the cell culture increased from 0.6 to 1.2 during decolorization). The presence of N,N-dimethylaminophenol, 4 methylaminophenol N, N,N-dimethylaminobenzaldehyde, [N, N-dimethylaminophenyl] [N-methylaminophenyl] benzophenone and N'-bis(dimethylamino) benzophenone (Michler's Ketone) was detected in their GC/MS analysis of crystal violet degradation products. These results suggest that crystal violet (CV) was biotransformed into Michler's ketone and N,N-dimethylaminophenol before being further degraded. Cytotoxicity and antimicrobial tests revealed that the decolorization process also detoxifies crystal violet.

In a related work, Singh and Singh (2010) employed Aspergillus flavus to biodegrade Congo red and Bromophenol blue, two commonly used textile dyes. In order to study the biodegradation of various colors by this fungus, Potato Dextrose Agar (PDA) medium was employed in each experiment. The amount of dye solution used in each experiment was set at 1.0% w/v. They reported that the fungus showed promising results for textile dye degradation. Dye degradation was seen in fungus-treated Petri plates as a change in the original color and a visible removal of color. The existence of color in the fungal mycelium or colored fungal mycelium in fungus-treated

Petri plates verified Singh and Singh's (2010) observation that dye degradation occurred when fungal mycelium accumulated colors.

In another study, Parshetti *et al*.(2006) investigated the decolorization of MG by *Kocuria rosea* . MG (50 mg/L) was completely decolorized by bacteria *Kocuria rosea* MTCC 1532 within 5 hours under static anoxic conditions, but no decolorization was observed under shaking conditions. Semi-synthetic media containing molasses, urea, and sucrose achieved 100, 91, and 81% decolorization, respectively, for the effect of nitrogen and carbon sources. According to Parshetti *et al*.(2006) induction of malachite green reductase and DCIP reductase activities during Malachite green decolorization suggests their involvement in the decolorization process. They also demonstrated that K. rosea could decolorize azo, triphenylmethane, and industrial dyes (cotton blue, methyl orange, reactive blue 25, direct blue-6, reactive yellow 81, and red HE4B).

In a separate experiment. Shedbalkar *et al*.(2008) investigated the decomposition of cotton blue dye. *Penicillium ochrochloron* decolorized cotton blue (50 mg/L) in 2.5 hours under static conditions at pH 6.5 and temperature 25 ºC. The ultimate products of cotton blue degradation, as determined by their Fourier Transform-IR spectroscopy and GC-MS analyses, were sulphonamide and triphenylmethane. They identified pH, temperature, and biomass maturity as factors influencing the rate of decolorization. Shedbalkar et al. (2008) also found that a rise in lignin peroxidase extracellular activity and the presence of aminopyrine N-demethylase, tyrosinase and lignin peroxidase activities in the cell homogenate indicate that these enzymes are involved in the decolorization process. Studies on the phytotoxicity and microbiological toxicity of extracted metabolites show that they are less harmful.

Khehra *et al.*(2005) conducted another study to enrich and isolate bacterial strains capable of decolorizing azo dyes present in soil/sludge samples collected from waste disposal sites of local textile industries. They isolated *Bacillus cereus* (BN-7), *Pseudomonas putida* (BN-4), *Pseudomonas fluorescence* (BN-5), and *Stenotrophomonas acidaminiphila* (BN-3) capable of completely decolorizing C.I. Acid Red 88 (AR-88), and used them to form the HM-4 consortium. The scientists also noted that whereas individual cultures took more than 60 hours to completely

decolorize the additional dye, the combined metabolic activity of the isolates allowed AR-88 (20 mg/L) to be completely decolored in just 24 hours. They also tested the consortium for its ability to decolorize different concentrations of other commonly used azo dyes, in addition to AR-88, and discovered that it could decolorize 82% of C.I. Reactive Red 120 ; 99% of C.I. Acid Red 119, 97; 99% of C.I. Acid Blue, 113; 94% of C.I. Acid Red, and 78% of C.I. Acid Red 88 dyes in 24 hours at an initial concentration of 60 mg/L of the mineral salt medium.

Employing thirty-nine strains of ligninolytic micro-organisms (fungi), Novotny et al. (2004) examined the degradability of Cu-phthalocyanine, anthraquinone, and azo dye structures and discovered that 60% of the dyes were susceptible to attack whereas 80–90% of the other dyes were. They reported that Irpex lacteus could decolorize a variety of phthalocyanine, thiazine, anthraquinone, triphenylmethane and azo dyes in stationary liquid culture at a concentration of 200 mg/L. After two weeks, their decolorization levels ranged from 60 to 100 %. Novotny *et al* discovered that sodium azide and n-propyl gallate selectively inhibited manganese-dependent peroxidase (MnP) and laccase, indicating that MnP is involved in the decolorization of anthraquinone- and azo dyes. I. lacteus decolorized 100% of Remazol Brilliant Blue R (150 mg/L) immobilized on pinewood cubes in six days. They also found that I.lacteus effectively removed color from textile industry effluent including Acid Black (AB), Drimarene Red (DR), Remazol Green (RG), and Drimarene Blue (DB), with corresponding decolorization rates of 35 %, 80%, 45%, and 100 % in 3-5 days.

Significant benefits of the method are its low cost, low operational costs, and non-toxic nature of the final products from complete mineralization. The main drawbacks of microbial treatment include low dye biodegradability, less flexibility in design and operation, a greater land area requirement, and longer times required for decolorization-fermentation processes, making it incapable of continuously removing dyes from effluent in liquid state fermentations despite the cost-effectiveness of this methodology and its suitability for a wide range of dyes.

### 2.3 Electrochemical Method

Electrochemical degradation is a method of converting organic compounds into other compounds by using direct oxidation and indirect oxidation processes. Harsini *et al.*(2016) investigated the

electrochemical degradation of malachite green in the presence of nanoporous carbon paste as the anode and silver wire as the cathode. Their findings revealed that the optimum state of degradation is 10 volts potential with an electrolyte solution of 0.1 M NaCl and pH does not affect degradation results. According to this study, the optimum time to degrade 50 ppm malachite green is 30 to 40 minutes to produce a harmless compound that can be determined by the impairment COD (95.05 %). Their UV-Vis spectra also confirmed that malachite green had been degraded.

Kusuma *et al.*(2016) investigated the degradation of malachite green dye using a voltage source potential with a defined current passed through carbon/$TiO_2$ electrodes as anodes and silver electrodes as cathodes. In a malachite green solution containing 0.1 M NaCl electrolyte support, degradation was performed with variations in potential, pH, and time. They obtained optimal conditions of pH 7-8 and a potential of 10 V after 15 minutes of degradation. Kusuma *et al*., (2016) concluded that the reactions that occurred were electrochemical-chemical-electrochemical (E-C-E) and irreversible based on the voltammogram. During 30 minutes, they also observed a reduction in the COD value of up to 81.89 % and 100 % degradation of malachite green solution at 25 ppm.

In a similar study, Chen *et al.,* (2020) investigated the efficient electrochemical degradation of Malachite green using Fluorine Doped Tin Oxide conductive glass as the anode. They investigated several factors influencing electrochemical degradation efficiency, including solution pH, electrolyte, applied current density, and degradation time. Chen *et al* used response surface methodology (RSM) for optimal conditions based on the results of a single-factor experiment. They discovered that electrolysis in 6.56 g/L NaCl (pH 8.84) solution with a current density of 8.61 $mA/cm^2$ for 20 minutes results in MG degradation rate exceeding 98 %. UV-VIS spectroscopy, fluorescence spectrometry, and total organic carbon analysis were used for the preliminary investigation of the degradation process. Miao *et al.,* (2020) investigated the effects of several experimental parameters, such as current density, pH, and supporting electrolyte, on the electrochemical oxidation of malachite green (MG) in a one-compartment batch reactor with a boron-doped diamond (BDD) anode and a stainless-steel cathode. They found that a current density of 32 $mA/cm^2$, a strongly acidic pH (pH = 3), and $Na_2SO_4$ as a good supporting electrolyte were the best conditions for degradation. Miao *et al*.(2020) also discovered that after 60 minutes

of electrolysis, a degradation efficiency of 98% was obtained, and 91% of chemical oxygen demand (COD) was removed after 180 minutes of electrolysis.

In a separate study, Bromophenol Blue (BPB) was used as a simulated pollutant while Zhang *et al.*( 2019) assessed the electrochemical performance of a porous $PbO_2$-$ZrO_2$ composite electrode. During the electrochemical degradation process, they optimized operating parameters including the supporting electrolyte ($Na_2SO_4$) concentration, initial pH values, current density and starting BPB concentration According to their findings, the COD and BB removal efficiency could reach 74.7% and 96.9%, respectively, after 90 minutes of electrolysis when the starting BPB concentration was 30 mg/L, the current density was 40 $mA/cm^2$, the pH level was 4, and the $Na_2SO_4$ solution concentration was 0.07 mol/L. Additionally, their kinetic curves showed that the pseudo-first-order process that caused the electrochemical breakdown of BPB had strong correlation values (R2 > 0.99). According to Zhang et al., the supporting electrolyte had the least impact on the electrochemical process, with the starting BB concentration and applied current density having the most effects. A few intermediates were created throughout the degradation process, according to high-performance liquid chromatography and the study of the ultraviolet-visible spectra. After 90 minutes of electrochemical deterioration, BB and intermediates were nearly entirely eliminated.

Similarly, Rong (2015) investigated the electrochemical anodic oxidation of bromophenol blue using boron-doped BDD as the anode. They used factorial design analysis to investigate the effect of statistically important operating parameters on treatment performance, such as treatment time, flow rate, applied current, and supporting electrolyte concentration. They believe that BDD technology is extremely effective in the treatment of bromophenol blue. Furthermore, the results demonstrated the applicability and potential of factorial design analysis in optimizing operating parameters and practical engineering applications of BDD technology (Rong, 2015).

This approach is efficient for decolorizing soluble and insoluble colors while lowering chemical oxygen demand. It is worth noting that, among other things, the rate of color and organic load removal is affected by the anode's composition and operating potential. However, the primary

disadvantages include high power costs and sludge generation, as well as contamination from chlorinated organics and heavy metals caused by indirect oxidation.

### 2.4 Microbial Fuel Cell

MFC is a biochemically catalyzed system that produces electricity by oxidizing biodegradable organic matter in the presence of fermentative bacteria or enzymes. Adeleye and Okorondu (2015) explored the creation of bioelectricity utilizing a microbial fuel cell and waste water from dorms for students. The Microbial fuel was created using two-liter plastic translucent chambers to replicate the fuel cell's two chambers, carbon and copper electrodes, 1% sodium chloride, and 2% agar proton exchange membrane. According to Adeleye et al. (2015), the starting voltage for both fuel cells throughout the 14 days was 308 mV and 338 mV, respectively, with a high of 0.81 V and 0.62 to 0.02 V for the copper-copper and carbon-carbon fuel cells, respectively. The voltage generation followed a conventional growth curve, with the consistency of the copper-copper fuel cell surpassing that of the carbon-carbon fuel cell. Additionally, they found that connecting the two fuel cells in series resulted in a total voltage of 138 mV (1.38 V), demonstrating that this configuration delivered the maximum output. Aerobic and anaerobic bacteria, such as Micrococcus spp., Corynebacterium spp., Staphylococcus spp., Enterococcus spp., and, Bacillus spp., were present on both electrodes.

Subsequent studies by Anuforo *et al.*(2017) evaluated the viability of producing bioelectricity from piggery wastewater. They used three 2-chamber MFCs with copper-copper (CuCu), carbon-copper (CCu), and carbon-carbon (CC) electrodes and piggery effluent with BOD levels of 420 mg/L and COD levels of 1057 mg/L. The authors measured the highest open circuit voltage (OCV) for CC, CCu, and CuCu, respectively, at 969.6 mV, 1228.5 mV, and 1338.5 mV. The voltage recorded across the MFCs was found to decrease as the external resistance decreased. The highest power density (at $R_{ext}$ = 1000) for CuCu, CCu, and CC were 92.29 $mW/m^2$ (114.0 $mA/m^2$), 156.32$mW/m^2$ (148.4 $mA/m^2$), and 79.27 $mW/m^2$ (105.7 $mA/m^2$), respectively. Across each MFC, power density increased as external resistance decreased until 200, at which time it declined. Anuforo *et al.*, (2017) discovered that after 25 days of operation, the coulombic efficiency of the Microbial fuel cell was 69 %, 74 %, and 84 %, respectively, while COD removal was 65 %, 47 %, and 51 % for CC, CuCu, and CCu. They also discovered that a carbon-carbon electrode mix

performed better in terms of electricity generation and wastewater treatment than copper-copper electrodes or their combinations. The pre- and post-isolation and identification of bacteria indicated the presence of *Lactobacillus species*, *Streptococcus species*, *Proteus mirabilis*, *Escherichia coli*, *Bacillus species*, *Corynebacterium species*, *Aeromonas species*, *Micrococcus luteus species*, *Pseudomonas species* and *Enterobacter species*.

In a related work, Liu *et al.*(2004) used a single-chamber microbial fuel cell with eight graphite electrodes (anodes) and one air cathode to evaluate power generation during wastewater treatment. Their system produced electricity (up to 26 $mWm^{-2}$) while eliminating up to 80 % of the COD from the wastewater when it was operated in continuous flow mode using primary clarifier effluent from a neighboring wastewater treatment facility. They discovered that the power output was proportional to the hydraulic retention time (3-33 h) and the influent wastewater strength (50-220 mg/L COD). The efficiency of the cathode was the primary determinant of the current generation. The system's coulombic efficiency, based on COD removal and current generation, was 12%, according to the authors, and the cathode performance was best when passive rather than forced air flow was allowed (4.5-5.5 L/min). This indicates that a sizeable portion of the organic matter was lost without current generation.

In a different study, Venkata Mohan *et al.*(2008) investigated the bioelectricity production of aerated and ferricyanide catholyte in a dual-chambered microbial fuel cell (MFC) (mediator less anode; graphite electrodes) using selectively enriched $H_2$-producing mixed consortia as anodic inoculums. Their results showed that in situ bioelectricity generation and wastewater treatment were feasible. They found that ferricyanide catholyte (586 mV; 2.37 mA; 0.559 kg COD/$m^3$ day) produced more power and removed more substrate than aerated catholyte (572 mV; 1.68 mA; 0.464 kg COD/$m^3$ day). At 100-ohm resistors containing ferricyanide and aerated catholyte, respectively, they found the maximum power yield (0.635 W/kg CODR and 0.440 W/kg CODR) and current density (222.59 mA/$m^2$ and 190.28 mA/$m^2$).

Similar to this, Pramanik and Rana (2017) looked at the viability of producing bioelectricity using a microbial fuel cell (MFC) that had a cation exchange membrane, carbon felt electrode and

mixed culture inoculation. The complete cell operation was tracked for up to 25 days while their cell was run under four external loads with pH levels varying from 4 to 10. The authors' findings showed that when hexacyanoferrate (III) was utilized as a cathodic reaction and the medium pH was neutral, it was possible to produce the most current and power. They recorded a maximum current density of 2.5 $Am^{-2}$, a power density of 1410 $mWm^{-2}$ on day 25, anode potential of -378 mV, and constant and consistent power from day 22 to day 25 when the cell was operated with 250 external loads. As operating duration rose, the fuel cell's internal resistance dropped, resulting in a columbic efficiency (CE%) of 22.70 % at the stable stage of operation.

### 2.5 Combined Process

Several attempts have recently been made to develop new combinations for effective wastewater treatment. Mohanakrishna *et al.* (2021) assessed the feasibility of combining electrochemical and bio-electrochemical systems to treat produced water in an energy-efficient manner. They employed five different current densities in the separate EC trials (4 h) (26, 36, 48, 59, and 71 $mA/cm^2$), and the effluents from each EC operation were then further processed by MFC (10 h) to generate bioelectricity. They observed that the extent of bioelectricity generation depended on the electrochemical oxidation of the electrochemical cell (EC) process and the overall maximum power generation of 2.74 mW was registered with EC-effluent from 48 $mA/cm^2$. Their integration showed the highest Total Produced Hydrocarbon (TPH) removal efficiency of 89% (EC, 305 mg/L; MFC, 317 mg/L) and COD removal efficiency of 89.6% (EC, 2160 mg/L; MFC, 1960 mg/L) at 71 $mA/cm^2$. The researchers also noted that the integration resulted in an overall net power production of 565 mWh (350 mL of anode capacity).

In a similar study, Zou and Wang ( 2017) also investigated the feasibility of azo dye wastewater treatment and simultaneous electricity generation in a novel electrolysis cell-microbial fuel cell process. They reported excellent Methyl Red removal and electricity production performance, with COD removal and decolorization efficiencies of 89.3 % and 100 %, respectively, and a 0.56 V cell voltage output. The decolorization rate (DR) was positively influenced by electrolysis voltage, while the current efficiency (CE) suffered a sharp decline. Although the COD removal rate in the EC system was only 38.5%, the biodegradability of the MR solution was much enhanced, with an

average DR of 85.6%. According to Zou and Wang (2017), the COD removal rate in the EC-MFC integrated process was 50.8 % higher than in the single EC system. Tawfik *et al.*, (2014) looked into the use of cationic polymer (Organo Polymer) in conjunction with a downflow hanging sponge (DHS) system in the treatment of reactive dye wastewater. At the ideal circumstances of hydraulic retention time (HRT) of 5 hours and 2.8 g COD/L.day organic loading rate (OLR), this combination method eliminated 90.12 % of the color and decreased COD by 66.5 %. The advantages of this combination process include high organic loads, minimal washout or clogging problems, a lengthy biomass retention time, and a small reactor architecture.

El-Gohary and Tawfik (2009) investigated the efficacy of a coagulation/flocculation (CF) and sequencing batch reactor (biological) combination in removing color and COD from industrial textile wastewater. They compared the color removal efficiency of magnesium chloride ($MgCl_2$/CaO) to that of alum and lime [$Al_2 (SO_4)_3$] (Cao). They discovered that adding magnesium chloride to the coagulation-flocculation process removed 100% of the color and reduced COD by 50 %. ($MgCl_2$). Furthermore, COD was reduced by 100% after the combined process with a sequential batch reactor (SBR).

In a separate study, Lu *et al.* (2009) treated reactive brilliant red X-3B wastewater with a combination of ozonation and up-flow biological aerated filtration (UBAF). They discovered that while ozonation was extremely effective at decolorizing the azo dye X-3B, it was less effective at reducing COD. The color removal and COD reduction efficiency were 97% and less than 30%, respectively, under optimum circumstances.The subsequent UBAF process, according to Lu *et al.*, (2009) significantly reduced the COD of wastewater treated with ozone pre-oxidation. On average, the UBAF process reduced COD by more than 85%. The ozone pre-oxidation process significantly improved the biodegradability of azo dye reactive brilliant red X-3B-containing wastewater, increasing the BOD5/COD value from 0.102 to 0.406.

According to de Souza et al. (2010), the use of ozonation to treat dye effluent led to the creation of by-products that were carcinogenic. After ozonation was implemented, a biofilm was used as a biological therapy to deal with the problem. Their toxicological research with Daphnia magna

showed that ozonation increased toxicity whereas biological treatment with a biofilm of the Remazol Black B dye effluent decreased it. As a result of using less ozone to break down the dye molecules, Souza et al. (2010) also came to the conclusion that the combined approach enhanced color removal while being more cost-effective.

Despite being a cost-effective and ecologically benign method, traditional biological degradation should not be employed as a stand-alone process to treat dye wastewater with high biotoxicity and poor biodegradability. In addition to having a high energy need and operating expense, electrochemical procedures are likely to produce secondary pollution from dye breakdown intermediates, which are frequently mutagenic, carcinogenic, or teratogenic. Finally, wastewater treatment methods will continue to evolve, with the development of more hybrid methods with high degradation efficiency. This is precisely what this review of the literature demonstrates. These various combinations present their own set of challenges in terms of cost, usability, accessibility, complexity, and power generation. As a result, more research is required to develop a net energy waste-water treatment process that is highly efficient, low-cost, simple, and easily accessible.

# CHAPTER THREE

# MATERIALS AND METHODS

This chapter covers materials and experimental approaches for this research work. It includes materials preparation (section 3.1) as well as a list of chemicals and reagents. This chapter also describes the preparation of MG and BB solution, culture media, and samples (section 3.1.2-3.1.5). Experimental procedure (section 3.2) electrochemical degradation experiments (section 3.2.1 - 3.2.5), Microorganism isolation, culturing and identification (section 3.2.6 - 3.2.9), microbial degradation experiment (section 3.2.10 - 3.2.11). An analytical procedure (section 3.3.13) involved in the research is a UV-Visible spectrophotometer. Computational studies of the pollutants (3.2.14), Sampling procedure, and data analysis are described as well in this chapter.

## 3.1 Material Preparation

### 3.1.1 Chemicals and Reagents

Bromophenol Blue and Malachite Green dye, supplied by Sinopharm Chemical Reagents Co., Ltd., were used as the contaminants. MacConkey Agar, Sabouraud Dextrose Agar, and Nutrient Agar, purchased from Sigma Aldrich, were used for the isolation and culturing of the microorganisms. Other chemicals and reagents used were of high quality and analytical grade.

### 3.1.2 Preparation Of Bromophenol Blue (BB) /Malachite Green (MG) Polluted Soil Sample

Soil samples (4.5 kg) were collected at a farm in SOSC extension FUTO. Then 1000 mL of 1g/L of BB/MG solution was added to the soil and left for 21 days.

### 3.1.3 Preparation of Culture Media

**MacConkey Agar**: One liter of deionized water was mixed with 52 grams of Mac Conkey agar powder. soaked for 10 minutes, then mixed, then sterilized for 15 minutes in an autoclave at 121 °C. The solution was combined and placed onto Petri dishes after cooling to 47 ºC.

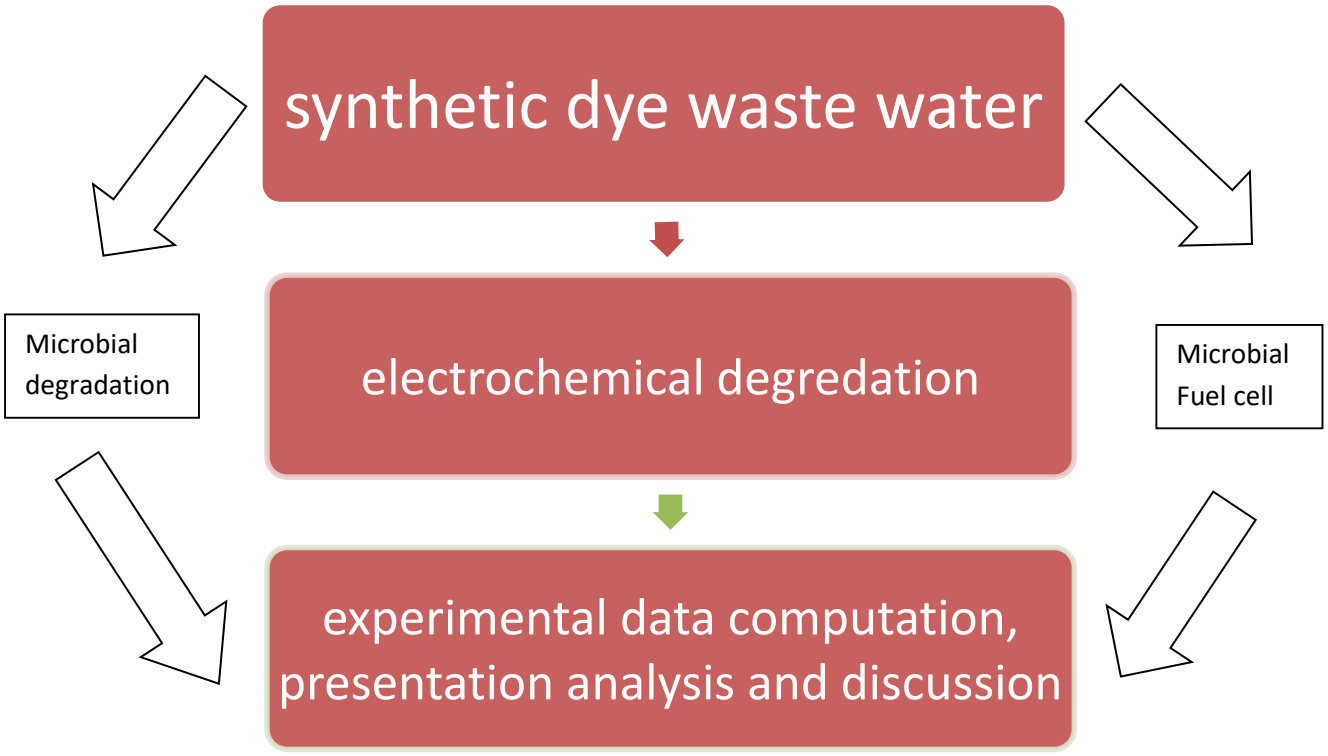


**Figure 3. 1 Workflow of the study**

**Sabouraud Dextrose Agar**: In 1 liter of distilled water, 65 grams of the powder were dissolved. The mixture was heated to 121 ºC for 15 minutes to thoroughly dissolve the medium before cooling to 45-50 ºC. It was then thoroughly combined and disseminated.

**Nutrient Agar:** In 1 L of distilled water, 28 grams of nutrient agar powder were dissolved. Swirled to thoroughly mix, then fully dissolved. The solution was autoclaved at 121 ºC for 15 minutes to sterilize it. The liquid was then transferred to a Petri plate and given time to set.

### 3.1.4 Preparation of MG Solution

The stock solution of 1000 ppm of Malachite Green solution was prepared by dissolving 1g of Malachite Green powder in 1L of distilled water. The solution was stirred continuously using a magnetic stirrer to ensure homogeneity.

$$C_a V_a = C_b V_b \qquad 0.1$$

### 3.1.5 Preparation of BB Solution

One gram of Bromophenol blue was dissolved in 1000 mL of distilled water to prepare 1 g/L of Bromophenol Blue solution. The solution was continuously stirred with a magnetic stirrer until it was completely dissolved. The stock solution was further diluted with distilled water to give the different concentrations.

$$C_1V_1 = C_2V_2 \qquad 0.2$$

## 3.2 Experimental Procedure

**Table 0.1 Experimental Variables**

| Variable | Values |
|---|---|
| pH | 3-11 |
| Current density | 0.27 – 1.33 mA/mm$^2$ |
| Temperature | 28-58$^0$C |
| Type of Supporting Electrolyte | KCl and NaCl |
| The concentration of Supporting Electrolyte | 0.005-1 M |
| Resistance | 100-330 ohms |
| The ratio of dye to the mineral salt | 1:2, 2:1 |

### 3.2.1 Degradation Experiment

An electrolytic cell with a 500 ml capacity was used to electrochemically decolorize BB/MG solutions. Ten ml of supporting electrolyte was added to 500 mL of 30ppm BB/MG solution and stirred with a magnetic stirrer for proper mixing. The Dc supply was set at 25V and desired current. Then Graphite plate anode and copper cathode of dimensions 60 x 25 x 2.5 mm are connected to the DC supply before being inserted into the electrolytic cell. The set-up is allowed to run for a

total of 110 min. about 3 ml of the sample is aspirated at 10 min intervals using a plastic syringe and taken for analysis (Oguzie *et al*., 2021).

### 3.2.2 Effect of pH on Electrochemical Degradation

By altering the solution's starting pH (3, 5, and 9) the impact of pH on the rate of degradation was investigated. Depending on the situation, either 0.1 M H2SO4 or 0.1 M NaOH was used to modify the pH. With constant stirring and dropwise addition of the acid/base, the pH was measured.

### 3.2.3 Effect of Temperature on Electrochemical Degradation

The effect of temperature on the degradation rate was studied by varying the initial temperature of the solution using a thermostat. The temperature was also monitored manually by a mercury bulb thermometer**.**

### 3.2.4 Effect of Supporting Electrolyte on Electrochemical Degradation

The effect of supporting electrolytes on degradation rate was studied by varying the type of electrolyte NaCl and the varying concentration 0.005, 0.1, 0.5, and 1 M. The same procedure is repeated for KCl.

### 3.2.5 Effect of Current Density on Electrochemical Degradation

The effect of current density on degradation rate was studied by varying the amount of current passing through the electrode for 1, 2, 3, 4, and 5A.

### 3.2.6 Preparation of Soil Sample

A ten-fold serial dilution as described by (Cheesbrough, 2004) was carried out. This was done by dissolving 1g of BB dye-polluted soil in a test tube in 9 mL of sterile water as a diluent (D1). Then 1 ml of diluent D1 was collected and added to another 9 mL of sterile water as a diluent (D2) in a test tube. A diluent factor of 10 (D10) was used in this serial dilution procedure.

### 3.2.7 Isolation and Identification

Following the serial dilution, triple inoculations of samples from diluents D5, D7, and D9 were performed on the three distinct medium. The inoculation was by the spread plate method of Cheesbrough (2004). Then, to produce pure culture for microbial identification, the microorganisms were streaked on a sterile Nutrient agar plate.

Identification was carried out according to Bergey's Manual of Determinative Bacteriology. The bacterial isolates were recognized and classified based on their morphological, cultural, and biochemical properties. Gram staining, $H_2S$ generation, Catalase, Oxidase, and Citrate utilization, motility, methyl red, sugar fermentation tests were run. Colonies with various morphologies were selected, and by further subculturing, they were cleansed.

### 3.2.8 Microbial Degradation Experiment

A volume of 100 mL of BB/MG and 50 mL of mineral salt medium were mixed in a conical flask. The isolated microbial strain was added to the mixture in a loopful. The experiment was carried out for nine weeks. 4 mL of the mixture is extracted once each week, centrifuged for 15 minutes at 4000 rpm, and then submitted for analysis. 100 mL of mineral salt and 50 mL of BB/MG dye are used for the procedure.

### 3.2.9 Effect of Dye and Mineral Salt ratio

The effect of mineral salt and dye volume on microbial degradation rate was studied by varying the ratio of dye and mineral salt combined i.e. dye volume: mineral salt volume for concentration 1:2 and 2:1

### 3.2.10 Pretreatment of Carbon Electrode and Nafion-117 Membrane

The electrodes were submerged in 0.5 M $H_2SO_4$ and deionized water for 20 min. and 24 hrs. respectively, to remove the metallic contaminant and equally increase conductivity. Thereafter, Nafion 117 sheet was arched to a size of 25 $cm^2$ and processed by boiling in a series of 30% $H_2O_2$, deionized water, 0.5M $H_2SO_4$, and deionized water for one hour each to improve porosity before use.

### 3.2.11 Microbial Fuel Cell Experiment (MFC)

H-type MFC made with two identical Duran bottles held together with external metal clamps was used for the setup. The anode and the cathode compartments were separated with a nafion 117 membrane About 25 ml of 50 ppm BB/MG dye and 50 mL of bacteria broth mixture was poured into the anolyte chamber while a mixture of 5mL of 0.1M, NaCl, and 75ml 0.1 M $KMnO_4$ was poured into the catholyte chamber. The carbon cloth (5x4x0.4 cm) anode and graphite sheet (5x4x0.4 cm) cathode were inserted into the chambers. Copper wire (0.4m long, 1.5mm) was used to connect the anode and the cathode, with a resistor placed in series between the anode and cathode. All exposed metal surfaces were sealed with a nonconductive epoxy resin. The setup was allowed to stand for 24 h before the open circuit voltage was recorded (Pramanik & Rana, 2017).

### 3.2.12 Effect of Resistance on MfC

By changing the resistor connected to the copper wire, the impact of resistance on the rate of degradation was investigated.The resistance adjustment was achieved by using 100 and 330-ohm resistors at different times.

### 3.2.13 Analytical Procedure

#### UV-Visible Spectrophotometer

The degradation of MG and BB was monitored using the UV-3600 Plus, a UV-Vis-NIR spectrophotometer equipped with specific detectors for different regions. The Photomultiplier tube (PMT) is utilized for the UV and visible regions, while the InGaAs and cooled PbS detectors cater to the near-infrared regions. A notable feature of the UV-3600 Plus, setting it apart from traditional spectrophotometers, is its employment of the InGaAs detector to cover the crossover region, ensuring enhanced sensitivity across the entire wavelength range of measurements. Impressively, it maintains a noise level of 0.00003 Abs at 1500nm. The instrument also boasts a high-performance double monochromator, facilitating the acquisition of precise data with an ultra-low stray-light level (0.00005% max. at 340nm) and a maximum resolution of 0.1nm. Moreover, its wide wavelength range, spanning from 185 to 3,300nm, enables comprehensive measurement

coverage across the UV, visible, and near-infrared regions (UV-3600i Plus Three-Detector UV-Vis-NIR Spectrophotometer, 2010).

The DE was examined from their absorbance (A) decay at the maximum visible wavelength of $\lambda_{max}$ = 590 nm for BB and 620 nm for MG and the percentage degradation was calculated and recorded using the：

$$\frac{A_{0-}A_t}{A_0} * 100 \qquad (3.3)$$

(Where $A_0$ and $A_t$ are the absorbances at time 0 and t respectively.)

### 3.2.14 Quantum Chemical Computation

BB/MG molecule's local reactivity was predicted using DFT simulations, which aimed to pinpoint the active regions in charge of the oxidative decolorization procedure. The goal of this work was to conceptually clarify the BB/MG decolorization mechanism. The Hirshfeld population analysis (Delley et al., 1990; Delley et al., 2000) and restricted spin polarization on the DND basis set were applied during the computational simulations, which made use of the DMol3 program (Materials Studio). Prior to carrying out these computations, a Smart minimization strategy with high convergence was used to geometrically optimize the BB/MG molecule structure utilizing the COMPASS force field (Oguzie et al., 2021).

# CHAPTER FOUR

# RESULTS AND DISCUSSION

This experiment examined the use of paired electrochemical and bio-electrochemical technologies to remediate water polluted with Bromophenol Blue (BB) and Malachite Green (MG) while simultaneously producing energy. An electrochemical oxidation procedure using copper cathode and graphite anode electrodes was employed for decolorizing MG and BB dye in an aqueous solution. Also, micro-organisms isolated and cultured from MG and BB dye-contaminated soil were employed for degrading BB and MG dye-contaminated water Bio-electricity was generated using BB and MG dye-contaminated water in a dual chamber MFC.

## 4.1 Microbial Degradation

To eliminate color from textile effluents, bacterial treatment offers a cost-effective and environmentally conscious alternative. In the experiments, the efficiency of local microorganisms in breaking down BB and MG was assessed over a period of nine weeks.

### 4.1.1 Identification of Micro-Organism

The identification of microbial strains involved the utilization of biochemical tests and examination of their morphological properties. Table 4.1 displays the codes and names of the isolated strains. From the contaminated soil with Malachite Green, five distinct isolates were obtained, whereas soil contaminated with Bromophenol Blue yielded seven distinct isolates as shown in the table below.

**Table 4. 1 Micro-organisms isolated from contaminated soil**

| Sample | Name of strain |
|---|---|
| M2 | *Eubacterium sp* |
| M3 | *Streptobacillus sp* |
| M4 | *Trichophyton Terrestre* |
| M5 | *Serratia marcescens* |
| MO2/M1 | *Aspergillus flavus* |

| | |
|---|---|
| BB1 | *Acinetobacter baumaniu* |
| BB2 | *Serratia marcescens* |
| BB3 | *Bacillus subtilis* |
| BB5 | *Bacillus megaterium* |
| BB6 | *Aspergillus niger* |
| BB7 | *Aspergillus Flavus* |
| BB8 | *Rhizopus stolonifera* |

The soil is a well-known habitat for micro-organisms and one of the largest sources of micro-organisms. Seven isolates were obtained from soil samples contaminated with Bromophenol Blue while 5 isolates were obtained from the soil sample polluted with Malachite green, that means all twelve isolates were resistant to 1000 ppm of studied dyes suggesting a natural adaptation of these isolates, as they were from dye- contaminated samples. Since micro-organisms need nutrients and other essentials to thrive in a habitat we can therefore say that the dye was toxic to other species of bacteria and fungi while the isolated ones thrived by using the dye as a source of the nutrient, a similar result has been reported by other authors (Bayoumi et al., 2014; Tayla *et al*., 2016). *Serratia marcescens* and *aspergillus flavus* isolates were both found in Bromophenol blue and Malachite green dye-polluted soil, meaning they can thrive in a variety of dyes ( Verma & Madamwar, 2003; Kang *et al.*, 2018;)

Some previous studies reported the ability of *Serratia marcescens* (Verma & Madamwar, 2003), *Aspergillus sp* (Kang *et al*., 2018), *Bacillus subtilis* (Kumar *et al.*, 2015), *Bacillus megaterium* (Joshi *et al*., 2013), *Rhizopus stolonifera* (Anand & Misra, 2017), *Eubacterium sp* (Shivangi *et al*., 2013), *Acinetobacter baumaniu* (Ning *et al*., 2014) for decolorization of textile dyes

### 4.1.2 Microbial Degradation of Bromophenol Blue and Malachite Green

The aim was to examine the degradation efficiency of Bromophenol Blue and Malachite Green using microorganisms. For this purpose, 50ppm of dye-contaminated water was inoculated with

the identified strains, each in a separate mineral broth.The results obtained are shown in Fig 4.1 and 4.2.

The plot in Fig 4.1 can be divided into two different regions. The first region depicts rapid degradation (the first 3 weeks) while the second region shows a steady degradation rate. Serratia marcescens achieved the highest degradation and in the fastest time of 2 weeks while Bacillus subtilis achieved the lowest. Generally, degradation efficiency increased as time increases.

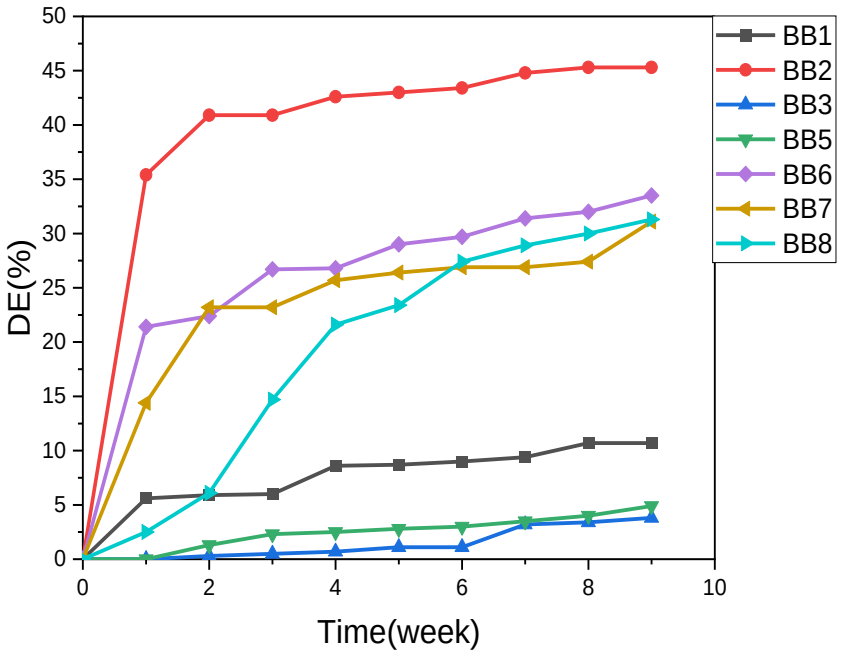


**Figure 4. 1 Graph showing the biodegradation efficiency of BB in 1:2**

**Legend: BB1, *Acinetobacter Baumaniu*; BB2, *Serratia marcescens*; BB3, *Bacillus subtillis*; BB5, *Bacillus megaterium*; BB6, *Aspergillus niger*; BB7, *Aspergillus flavus*; BB8, *Rhizopus stolonifer***

The graph in fig 4.2 shows that degradation efficiency increased with time. Trichophyton terrestre, Serratia marcescens, and Aspergillus flavus recorded a very fast degradation rate in the first week

and steadily increased in the following week. Eubacterium sp degradation efficiency can be described as a linear-steady-linear-steady profile. Streptobacillus sp did not degrade the dye until the 2nd week

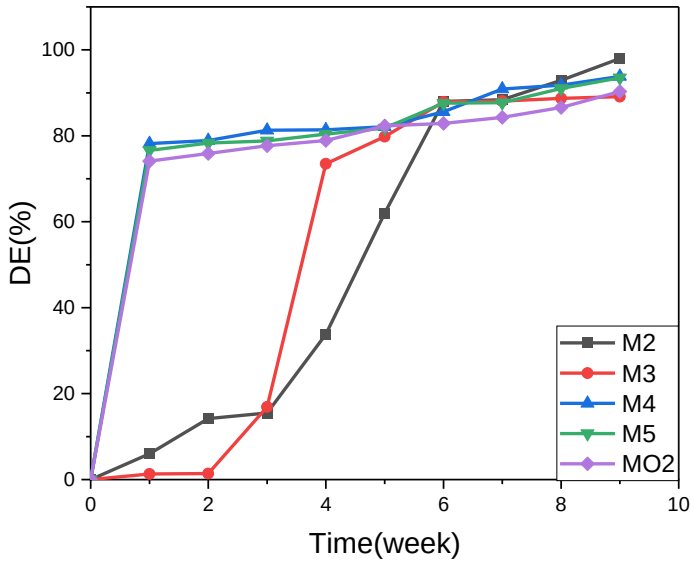


**Figure 4. 2 Graph showing the biodegradation efficiency of MG in 1:2**

**Legend: M2, *Eubacterium sp*; M3, *Streptobacillus sp*; M4, *Trochophyton Terrestre*; M5, *Serratia marcescens;* MO2, *Aspergilus flavus***

Biodegradation is defined as the biologically mediated breakdown of chemical compounds; it is a time-consuming process that entails the breakdown of dye into numerous byproducts by the activity of various enzymes (Kaushik & Malik, 2009). Biodegradation of synthetic dyes results not only in dye decolorization but also in the fragmentation of dye molecules into smaller and simpler pieces (breakdown products). Decolorization of the dye occurs when the dye's chromophoric center is cleaved, as evidenced by a progressive decrease in absorbance at the max (BB = 590 nm and MG = 620 nm). The microbial strains that were identified exhibited different capabilities in breaking down BB and MG dye-contaminated water. Certain microorganisms demonstrated notable advantages over others in the biodegradation of Bromophenol Blue and Malachite Green

pollutants. The efficacy of microbial decolorization relied on the adaptability and activity of the chosen microorganisms.

Dye decolorization can occur in two ways: adsorption on microbial biomass or biodegradation of the dyes by cells (Ali, 2010). Dye adsorption can occur on both living and dead microbial cells, preserving the original dye structure without breaking it down. On the other hand, biodegradation involves microbial cells breaking down the dye, leading to its fragmentation and, in some cases, complete mineralization into CO2, H2O, and simple organic compounds. The degradation of BB and MG primarily followed the biodegradation process due to the nature of both processes (biosorption and biodegradation). Dye biosorption does not provide a solution to the problem, as it only traps the pollutant within the adsorbent matrix (the microbial biomass) without eliminating it. Disposing of microbial biomass carrying adsorbed dyes presents a significant challenge in implementing bio-cleaning methods for colored waterways (Chander & Arora, 2007). A biosorption process, in addition to biodegradation, may play an essential part in the decolorization of dyes by a live fungus (Fu & Viraraghavan, 2001), and dye biosorption may be of importance in bio-recovery of these synthetic compounds from wasted dye baths. This is accomplished by desorbing the adsorbed dyes using appropriate solvents or solvent combinations (Ali, 2010).

### 4.1.3 Investigating the Impact of Dye and Mineral Salt Volume Ratio on the Microbial Degradation of Malachite Green and Bromophenol Blue

Degradation experiments were conducted using two distinct ratios of dye to broth solution to investigate how the efficiency of Malachite Green and Bromophenol Blue degradation is influenced by the concentration of both the dye and mineral salt. The plot of degradation efficiency as a function of micro-organisms is shown in fig 4.3 and fig 4.4

The plot in Fig 4.3 shows that Aspergillus flavus and Streptobacillus sp performed better in 2:1, Eubacterium sp and M4 performed better in 1:2 and Serratia marcescens performed well in both ratios. The micro-organisms also achieved very high degradation efficiency irrespective of their dye-to-mineral salt ratio

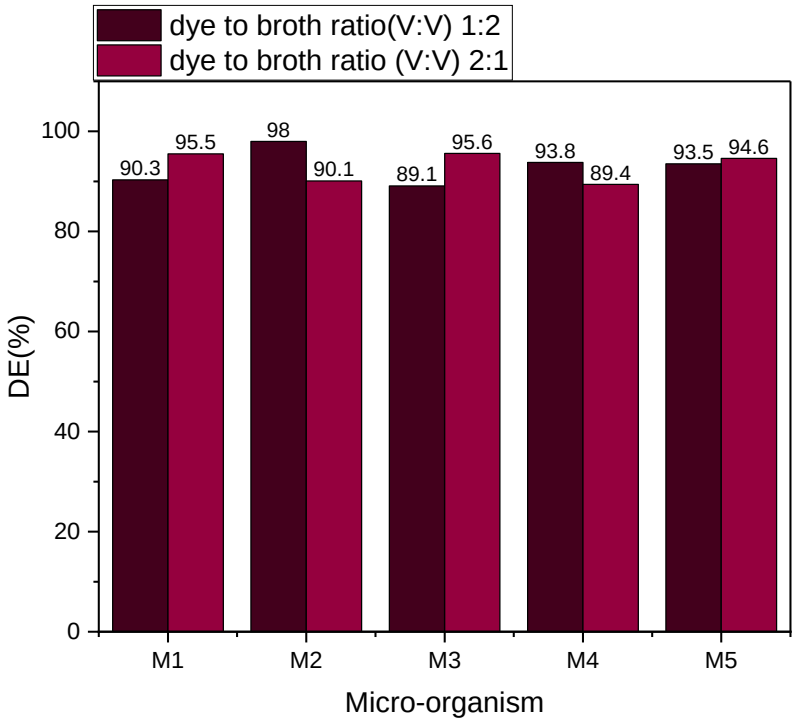


**Figure 4. 3 MG Degradation at Different Dye and Mineral Salt Volume Ratios**

**Legend: M2, *Eubacterium sp*; M3, *Streptobacillus sp*; M4, *Trochophyton terrestre*; M5, *Serratia marcescens;* MO2, *Aspergilus flavus***

The bar chart in fig 4.4 shows two distinct results. Acinetobacter baumannii, Serratia marcescens, Aspergillus niger, Aspergillus flavus, and Rhizopus stolonifer exhibited greater degradation efficiency at a ratio of 1:2 compared to 2:1. Conversely, Bacillus subtilis and Bacillus megaterium demonstrated consistent performance regardless of the dye/mineral salt ratio.

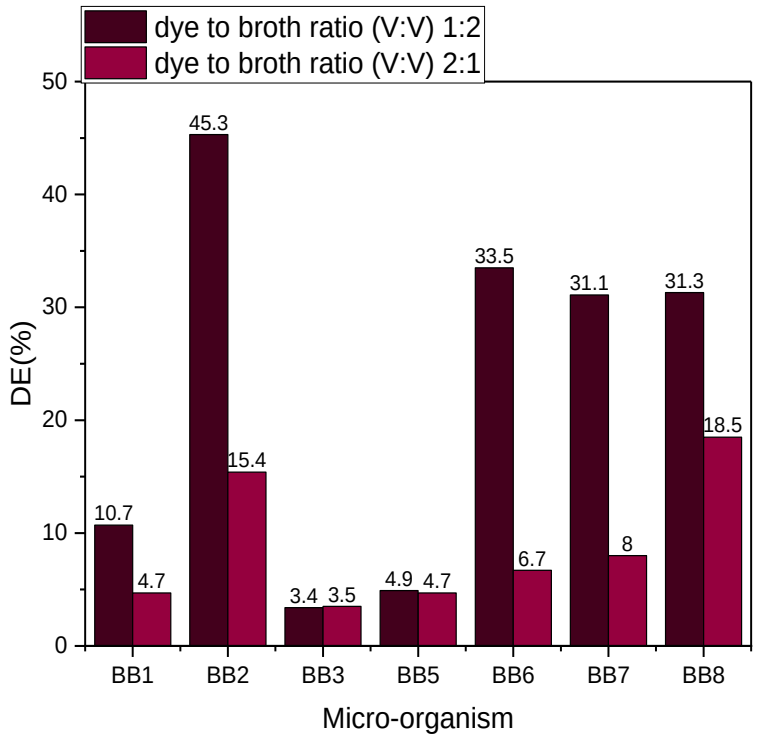


**Figure 4. 4 BB degradation at different dye to mineral broth ratio**

**Legend: BB1, *Acinetobacter Baumaniu*; BB2, *Serratia marcescens*; BB3, *Bacillus subtillis*; BB5, *Bacillus megaterium*; BB6, *Aspergillus niger*; BB7, *Aspergillus flavus*; BB8, *Rhizopus stolonifer***

Abiotic mechanisms and microbial metabolic activities have the greatest effect on pollutant decolorization. The ability of bacteria to breakdown synthetic colors have been connected to enzyme synthesis during degradation. The growth of microorganisms and their decolorization ability can be impacted by the presence of harmful dye levels. The dye's class, which determines its structural characteristics, also plays a role in the extent of decolorization. Additionally, the quantities of nitrogen and glucose in the medium can influence dye decolorization by affecting the bacteria's enzyme-producing capacity. Our findings align with this, as we observed that ratio 1:2 performed better than ratio 2:1. In this study, it was discovered that medium containing less Bromophenol Blue dye concentration and more mineral salt degraded faster. This is in agreement with studies carried out by ( Pazarlioglu *et al*., 2005; Parshetti *et al*., 2006; Parshetti *et al*., 2011;).

It was also observed that decolorization efficiency for degradation of Malachite Green contaminated water did not follow the rule but was an exception, as the dye to mineral salt ratio had little to no effect on the degradation efficiency of MG. A similar result was obtained by Olukanni *et al., 2021* who ascribed the cause to be because sometimes dyes act as inducers of enzyme production in a culture medium and are in turn decolorized by the enzymes, and the highest inducer is decolorized highest (Olukanni *et al.*, 2021)

### 4.2 MFC/Bioelectricity Production

The generation of electricity from MG and BB-contaminated water was carried out using indigenous cultured micro-organisms. Only the best performing micro-organism during bio-degradation was used in the MFC. In addition to the dye-contaminated water as a substrate for both fuel cells, potassium permanganate was used as the catholyte. The set-up was allowed to stand for 24hr before the initial reading was taken. The results for the open circuit voltage and current recorded are shown in fig 4.5 and fig 4.6

Fig.4.5 shows two very distinct phases i.e., high value (1-6th day) and low value (7 -14 th day) phases. A high OCV and OCA were recorded in the first four days with the highest obtained 0n 3rd day (1.5 V) and 2nd day (1.7mA) respectively, after which a decline in OCV and OCA followed.

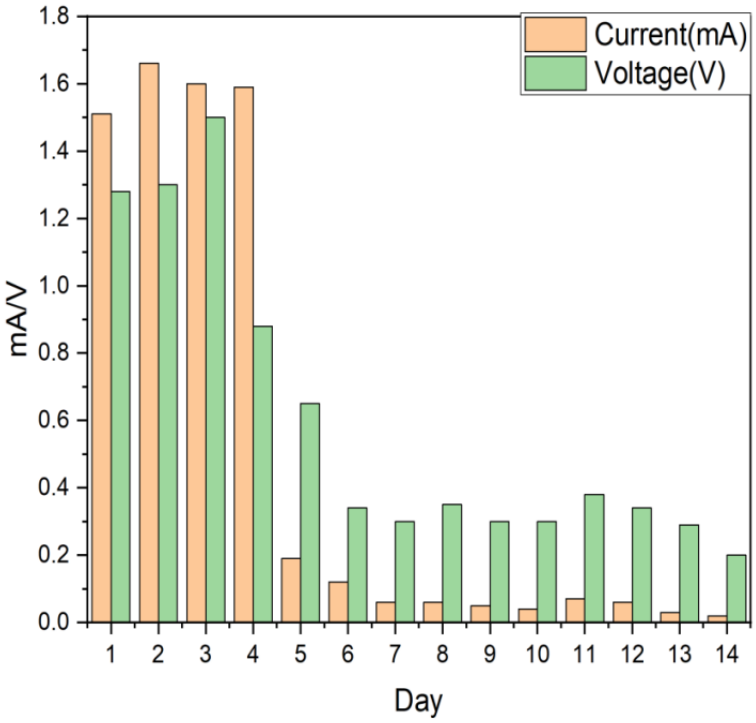


**Figure 4. 5 Plot for open-circuit voltage and current for MFC using Bromophenol Blue dye as substrate**

The plot in Fig.4.6 shows a very irregular OCV and OCA reading. Zero values were recorded for the first 2 days and no current was recorded from the 10th day. The highest voltage of 0.75V was obtained on the 6th day while the highest current was obtained on the 3rd day.

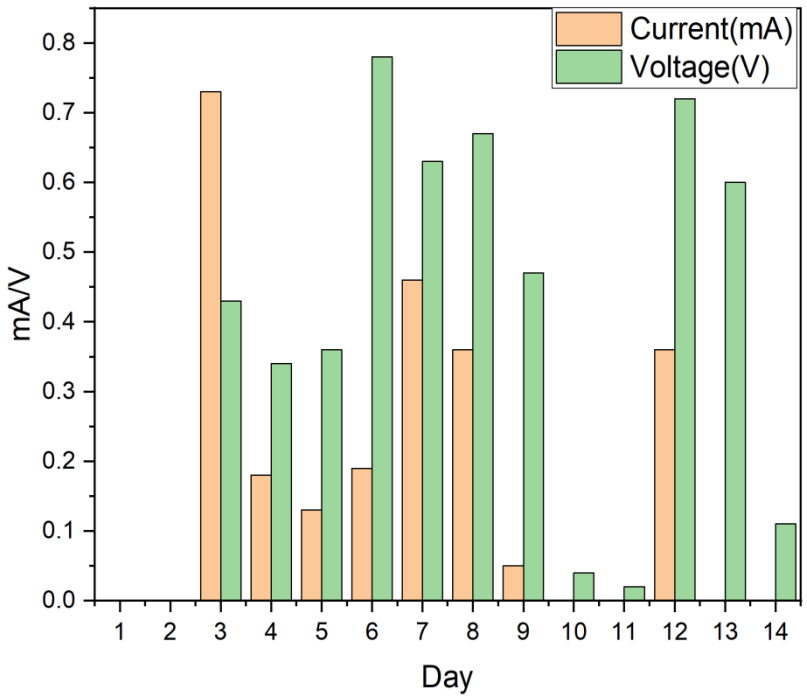


**Figure 4. 6 Plot for open-circuit voltage and current for MFC using Malachite Green dye as substrate**

According to Logan (2007), "in an MFC, the bacteria must colonize the electrode and create enzymes or structures necessary to move electrons outside the cell over time." In mixed cultures, various bacteria develop and reach distinct potentials. This explains why the experiment required such a lengthy acclimation time (24 hours for BB-based MFC and 72 hours for MG-based MFC). There is then an exponential development stage during which the organisms (electricigens) aggressively use the organics in the wastewater for energy which accounts for the peak period of voltage recorded. Later, close to the conclusion of the 14 days, the voltage started varying again. These were ascribed to the organisms' consumption of organic materials in the wastewater, accumulation of toxic compounds, and inter/ intra-species competition, which is why they are progressively approaching the decline phase of development (Adeleye & Okorondu, 2015). The fact that both MG and BB-based MFC could produce electricity shows that the injected

microorganisms were electro-active. Exoelectrogens are the most prevalent organisms linked to biofilm development (Shewa et al., 2013)

### 4.2.1 Effect of Resistance on Current Density

The current density of the microbial fuel cells (MFCs) across the two resistors was determined by correlating the voltages measured across known external resistors with the anode surface area. Ohm's law states that current (I) at constant voltage is inversely proportional to applied external resistance (R) (V).

**V = IR** **4. 1**

The resultant effect of resistance on current density as a function of time is shown in fig 4.9

From figure 4.7 it can be deduced that the 330-ohm resistor recorded a higher current density than the 100 ohms resistor on 2 different days (the 4th and 7th day) while on the 5th,6th, and 8th day the 100-ohm resistor generated a higher value than the 330 ohms. The maximum current density recorded across 100 Ω for MG was 92 mA/m$^2$ while 75.69 mA/m$^2$ and was the highest recorded across 330 Ω resistor for MG-based MFC. The maximum current density was recorded on the 4th day for 330 Ω resistors and the 5th day for 100 Ω resistors

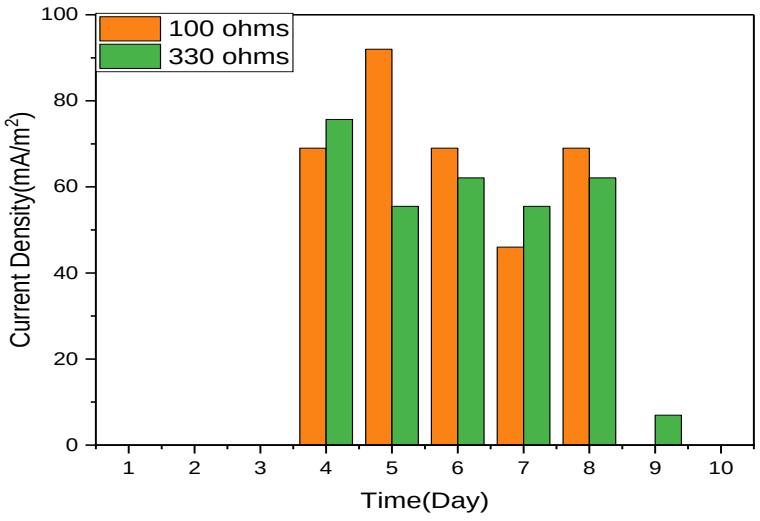


**Figure 4. 7 Current density across 100 and 330 Ω resistors in MG-based MFC**

Fig 4.8 shows two very distinct phases. The first phase shows relatively high and steady values for both 330 and 100 ohms resistors. The values generated for 100 ohms are generally higher than that of 330 ohms with the exception being on the 4th day. The maximum current density was recorded on the 4th day (341.74 mA/$m^2$) for the 330 Ω resistor and the 5th day (550 mA/$m^2$ ) for the 100 Ω resistor.

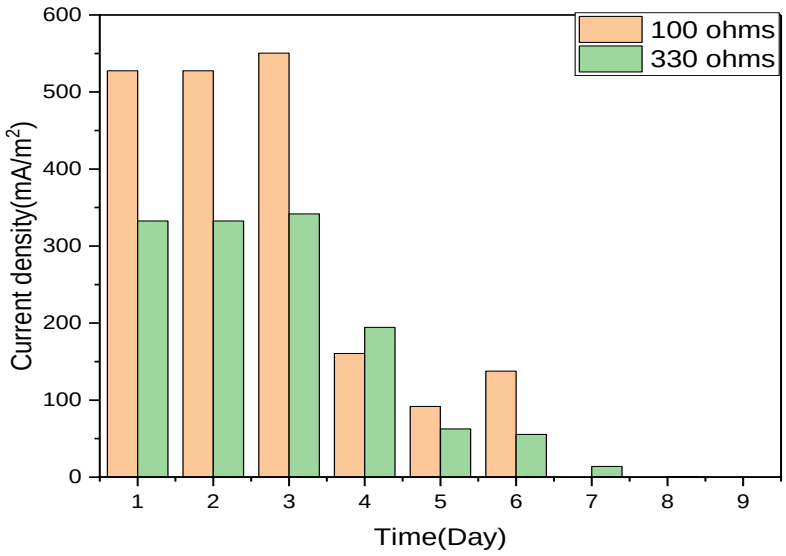


**Figure 4. 8 Current density across 100 and 330 Ω resistors in BB-based MFC**

Current density is the amount of charge per unit of time that flows through a unit area of a chosen cross-section. Current density is important to the design of electrical and electronic systems. Circuit performance depends strongly upon the designed current level, and the current density then is determined by the dimensions of the conducting elements. From the results, it can be deduced that current density increased with decreasing external resistance. This is in line with Ohm's rule, which stipulates that current rises as external resistance lowers at a constant voltage. simialr trend was also reported by other researchers (Taylor *et al*., 2014; Anuforo et al., 2017; Pramanik & Rana, 2017)

### 4.2.2 Power Density

The power derived from the MFC was calculated using the voltage measured across a known external resistor and the surface area of the anode.

**Power = $I^2$ x $R_{ext}$** **4. 2**

The resultant effect of resistance on the power density of microbial fuel is shown in fig 4.9 and fig 4.10.

Fig 4.9 shows a very irregular pattern for power density as a function of time. The power density associated with the 330 ohms can be best described in terms of high-low-high series. While the power density of the 100-ohm resistor increased from the 4th day, peaked on the 5th day, and reduced on the 6th day but increased again on the 8th day. The maximum power density for MG was recorded on the 5th day for 100 Ω resistors and the 4th day for 330 Ω resistors.

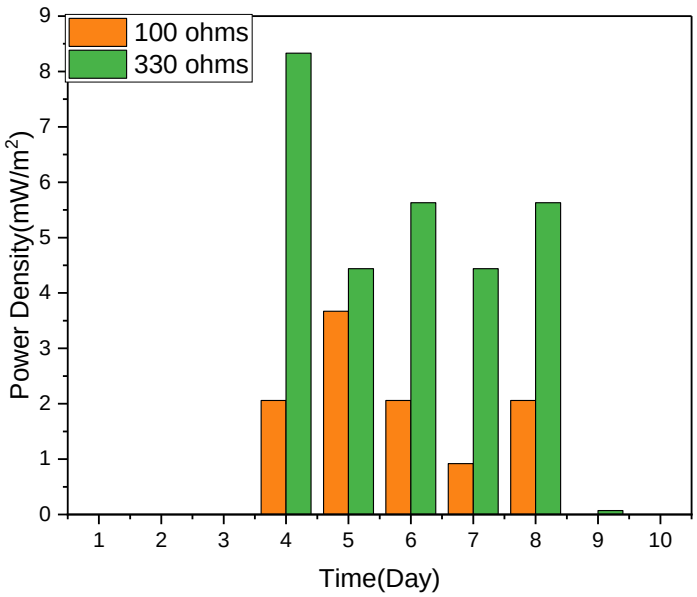


**Figure 4. 9 Power density across 100 and 330 Ω resistors in Malachite green-based MFC**

Fig 4.10 has 3 distinct regions. Days 1-3 recorded relatively high and steady current densities, day as average value, and days 5-6 recorded very low and steady current densities. The maximum power density for BB was recorded on the 3rd day for both 100 and 330 Ω.

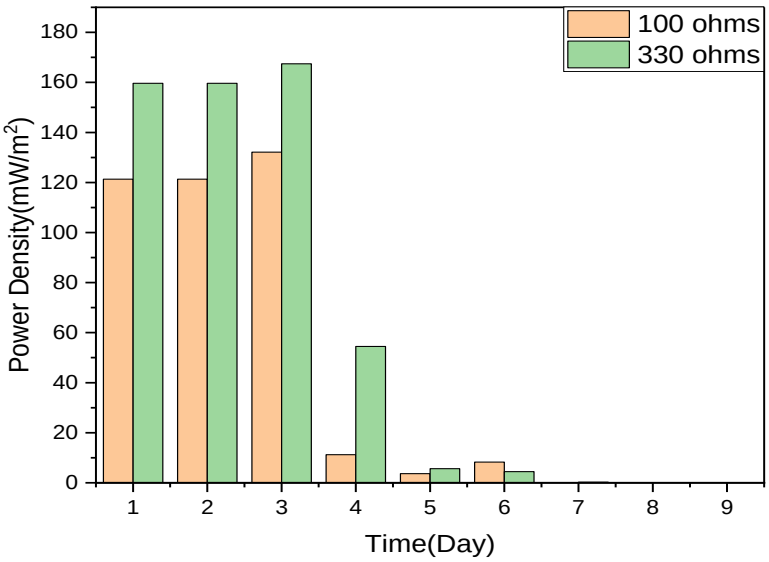


**Figure 4. 10 Power density across 100 and 330 Ω resistors in Bromophenol Blue-based MFC**

The value of power densities for 330 ohms is bigger than that of 100 ohms for BB and MG-based MFC. Therefore, we can say that power density increases with an increase in resistance. The max power density obtained from MG across 330 Ω was higher than that recorded by ( Liu *et al.*, 2009; Kalathil *et al.*, 2011, 2012) in their various experiments. The maximum power density obtained from BB was greater than that obtained from MG and conducted by (Sun *et al*., 2012) in their study of anode enlargement for enhanced simultaneous azo dye decolorization and power output in air cathode microbial fuel, but this is less than the maximum recorded by (Li *et al*., 2010; Sun *et al*., 2009, 2011; Hou *et al*., 2011 )

### 4.3 Electrochemical Degradation

#### 4.3.1 Effect of Initial pH Of Malachite Green and Bromophenol Blue Dye Solution

The efficiency of electrochemical degradation processes is greatly affected by the pH of the solution, with the optimal dye removal occurring at a specific pH level. To alter the pH of the dye solutions, 1 M H2SO4 or 1 M NaOH was utilized. Figure 4.11 and 4.12 present the degradation efficiency as a function of time at different pH levels.

In the shortest time of 20 minutes, pH 5 achieved more than 90 % degradation efficiency. The pH 11 profile differs slightly from the other pH levels. The pH pattern in the profile is linear rise-steady. The maximum degradation efficiency (98.5 %) was reached at pH 5, whereas the lowest degradation efficiency (73.5 %) was found at pH 11.

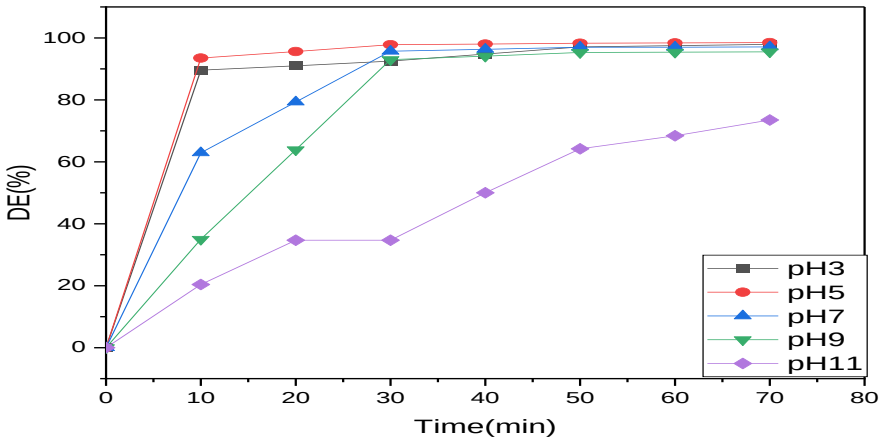


**Figure 4. 11 Effect of initial pH decolorization efficiency of MG**

*(Concentration = 30 mg/L, Current density = 1.33mA /mm$^2$, Temperature (T) = 28 $^o$C, Voltage = 25 V, Electrolyte = 1 M KCl)*

The degradation efficiency profile in Fig 4.12 can also be divided into two regions. A region of rapid linear growth for the first 40 min and a region of steady growth for the next 30 min. The maximum degradation efficiency was achieved at pH 3 (100 %) while the lowest degradation

efficiency was at pH 11(97 %). to reaction time; pH 3 achieved more than 90 % degradation efficiency at 30 min, pH7 at 40min, pH 9 at 50min, and pH 11 at 70min.

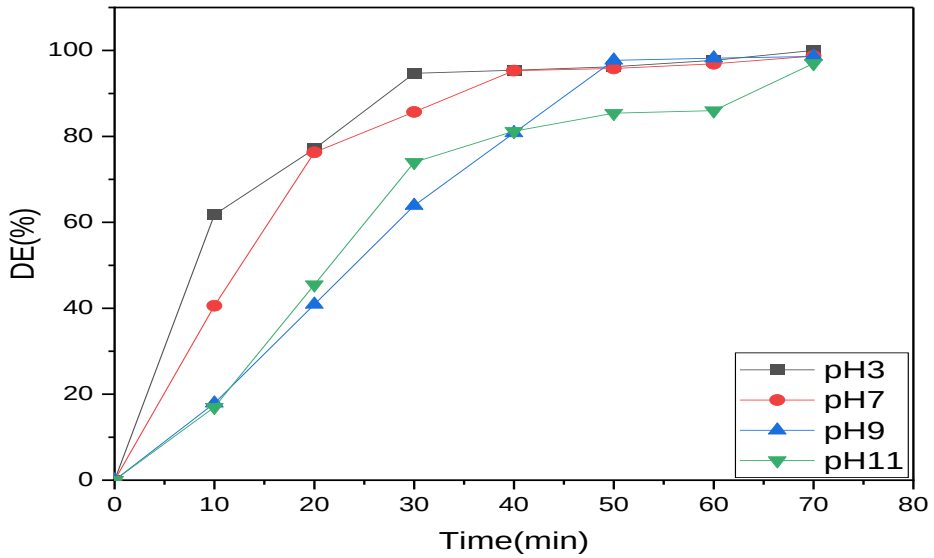


**Figure 4. 12 Effect of initial pH decolorization efficiency of BB**

*(Concentration = 30 mg/L, Current density = 1.33 mA /mm$^2$, Temperature (T) = 28$^o$C, Voltage = 25 V, Electrolyte = 1 M KCl)*

The initial pH of the solution is a critical factor that influences the advancement of electrochemical processes. Understanding the pH dependence of degradation processes can be complex as it impacts various properties, such as the chemical states of solution species and solvent molecules, electrostatic interactions at the electrode/solution interface, and the types of active oxidizing species generated during the reaction, among others (Oguzie et al., 2021). Within the anodic oxidation system, a continuous competition occurs between the reactions of oxygen evolution and the oxidative degradation of organic substances on the anode. As the solution's pH increases, the rate of oxygen evolution at the anode surface also rises. Consequently, this reduces the oxygen evolution potential, hinders the diffusion of organic pollutants to the anode, and ultimately decelerates the oxidation rate of organic matter on the anode surface (Zhao *et al*., 2019). On the

other hand, when the environment is acidic, the electrochemical conditions for organic pollutant degradation at the anode surface get better as the oxygen evolution process slows (Aquino Neto & de Andrade, 2009). Moreover, in alkaline conditions, the solution's conductivity decreases because of inadequate supporting electrolytes, leading to a further decline in the efficiency of decomposing organic pollutants (Dai *et al*., 2013). The considerably decreased decolorization efficacy at alkaline pH may be caused by the low oxidation potential of ClO species relative to $Cl_2$ and HOCl ( Rajkumar *et al.*, 2007; Kariyajjanavar *et al.*, 2011; Baddouh *et al*., 2018). The findings are in line with the results reported by (Reza et al., 2020), demonstrating that higher degradation efficiency is attained in the acidic medium for both MG and BB compared to the alkaline medium.

Therefore, pH 5 and pH 3 were the ideal conditions for MG and BB decolorization. Studies on the electrochemical degradation of methylene blue dye using a graphene-doped $PbO_2$ anode (Reza *et al*., 2020) and electrochemical degradation of Bromophenol blue on porous $PbO_2$-$ZrO_2$ composite electrodes (Reza *et al*., 2020) both came to the same conclusion that the optimal degradation occurred at pH 5.6 and 3 respectively. . Furthermore, the kinetics of contaminant removal at pH = 3 was greater than pH values of 7 and 10 in research by Fernanda *et al*. for the degradation of dimethyl phthalate ester employing fluoride-doped Ti/b- $PbO_2$ anode (Souza *et al*., 2014). Additionally, employing an Nb/$PbO_2$ anode, the maximum electrochemical breakdown efficiency of methyl Orange was attained at an initial pH of 6 (Zhao *et al*., 2019). All of the above experiments are in support the result of this study

### 4.3.2 Effect of Current Density

An important factor in regulating the rates of electrochemical processes is current density, which is a measurement of the number of electrons moving between the anode and cathode. At a very high voltage of 25 V, five different values of current density ranging from 0.27 $mA/mm^2$ to 1.33 $mA/mm^2$ were examined to evaluate the impact of current density on the effectiveness of electrochemical decolorization of BB and MG. The correlation between MG and BB degrading efficiency and current density are shown in Fig.4.13 and fig 4.14 respectively.

The plot in figure 4.15 can be divided into two regions. The first region from 0-20 mins shows rapid linear growth while 30-40 mins show steady growth. Additionally, Fig.4.3 demonstrates that current density at 1.33 mA/mm$^2$ achieved more than 90 % degradation in 10 min; 0.27, 0.53, and 0.8 mA/mm$^2$ did this in 30 min; and 1.33mA/mm$^2$ achieved this in 20 min. The effectiveness of removing MG dye increased from 96.7 % to almost 99 % when the current density was increased from 0.27 mA/mm$^2$ to 1.33 mA/mm$^2$.

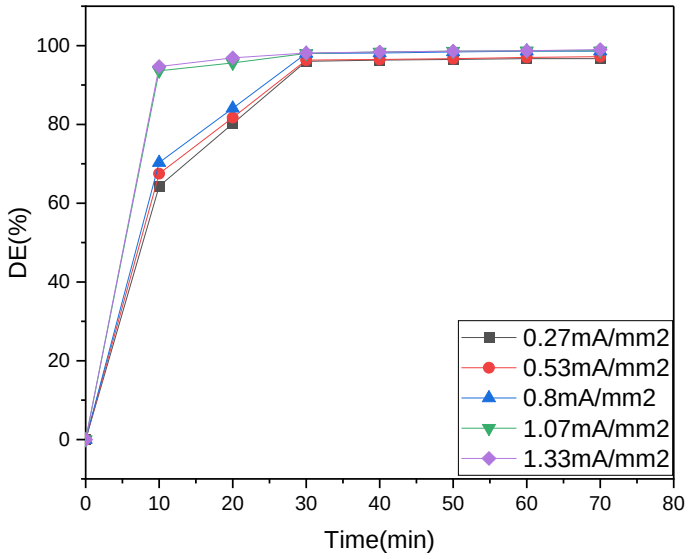


**Figure 4. 13 Effect of current density on decolorization efficiency of MG**

*(Dye concentration = 30mg/L, Temperature (T) = 28 $^o$C, Voltage = 25 V, Electrolyte = 1 M KCl, pH = 7)*

Figure 4.16 displays the anticipated pattern of enhanced degradation efficiency as the reaction time progresses.The plot also has two regions i.e rapid linear growth (0-30 min) and steady growth (40-70 min). For reaction time 1.33 mA/mm$^2$ attained more than 90 % degradation in the quickest time (10 min) when compared to other current densities. The highest degradation efficiency (99.9 %) was recorded at 1.33 mA/mm$^2$and the lowest (95.5 %) was recorded at 0.27mA/mm$^2$.

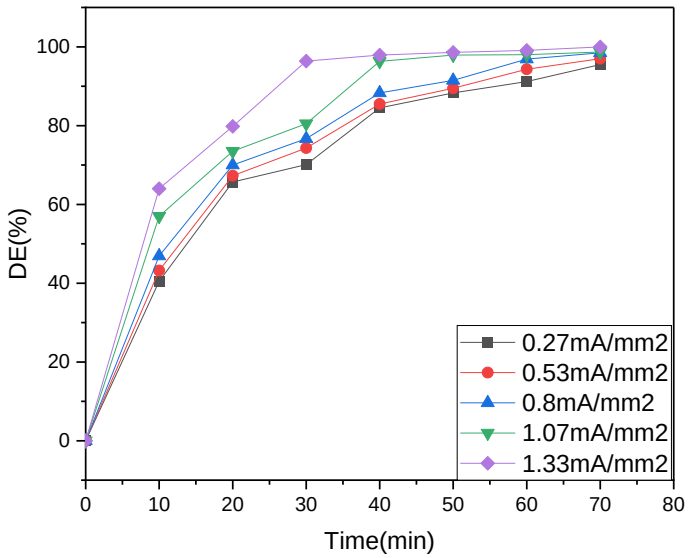


**Figure 4. 14 Effect of current density on decolorization efficiency of BB**

*(Dye concentration = 30mg/L, Temperature (T) = 28 $^{o}$C, Voltage = 25 V, Electrolyte = 1 M KCl, pH = 7)*

Among the factors influencing the electrochemical oxidation process, current density has been identified as one of the most critical factors responsible for regulating the rate of electrochemical degradation (Ansari & Nematollahi, 2018; Nakamura *et al*., 2019). Increasing the current density over a fixed duration enhances electrochemical oxidation systems' efficiency by speeding up the synthesis of HO and water oxidation at the anode surface ( Wang *et al*., 2015; Dai *et al*., 2016). Contrarily, using a greater current density in the electrochemical cell stops the electrolysis intermediates from deactivating the electrochemically active sites on the anode surface. However, a significantly higher current density might exacerbate the immediate and unfavorable effects of oxygen evolution at the anode surface, which competes with the oxidation of organic matter there and, ultimately, lowers the effectiveness of organic pollutant removal in electrochemical degradation systems ( Wang et al., 2015; Ansari & Nematollahi, 2018; Yao et al., 2019). Because of this, the degradation of the MG and BB dyes in this investigation was beneficial at high current densities between 0.27 and 1.33 mA/mm2. This was supported by (Zhao *et al*., 2019). In addition, Duan *et al., 2013* investigation for the electrochemical degradation of phenol by lead dioxide

anode showed that increasing the current density in the 10–50 mA/cm$^2$ range led to an increase in phenol elimination effectiveness from roughly 19 % to 79 % (Duan *et al*., 2013).

### 4.3.3 Influence of Supporting Electrolyte

The objective of the experiments was to evaluate how varying concentrations of two supporting electrolytes (KCl and NaCl) influence the efficiency of MG and BB decolorization.The acquired findings for KCl and NaCl after 70 minutes of exposure are shown in Figs. 4.15 and 4.16, respectively.

From Fig 4.15 it can be seen that 1M NaCl behaved differently from other concentrations. the 1M NaCl concentration achieved a very fast degradation efficiency of 80 % in 10 mins and steadily increment for the next 60 min. concentration 0.5, 0.1, and 0.05 M followed the same pattern of slow linear color decolorization. 1 M achieved the highest degradation efficiency of 98.3 % while 0.05 M recorded the lowest (38.1 %).

Also, from fig 4.15b, it can be seen that 1M KCl and 0.5 M have a different profile from the other concentrations. 1 M KCl achieved 90% degradation efficiency in 10 min and steady growth. The 1 M and 0.5 M degradation profiles can be described as a steep linear degradation curve from the 10$^{th}$ min to the 50th min while the other two concentration profile is a very low steep growth. 1 M concentration achieved the highest degradation of 99 % while 0.05 M recorded the lowest degradation efficiency of 17.6 %. With a rise in both KCl and NaCl concentrations, both graphs demonstrate an increase in degradation efficiency. Fig 4.17 also shows that KCl achieved higher degradation than NaCl.

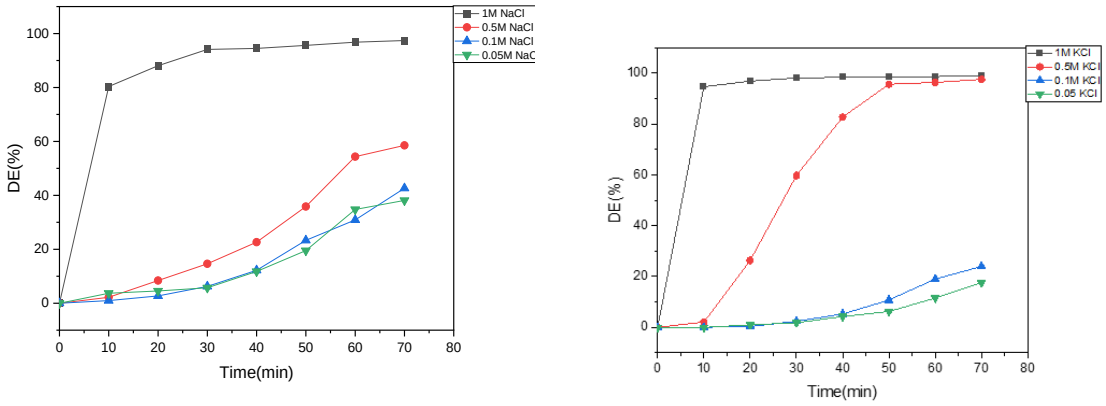


(a) (b)

**Figure 4. 15 Effect of supporting electrolyte on decolorization efficiency of MG using (a) NaCl and (b) KCl**

*(Dye concentration = 30 mg/L, Temperature (T) = 28 $^{o}$C, Voltage = 25 V, Electrolyte = 1 M KCl, Current density = 1.33 mA/mm$^{2}$)*

From figure 4.16a it can be seen that the DE curve for 1M and 0.5M concentrations differ from that of 0.1 and 0.05M. The first 50 min for both 1M and 0.5M shows a very steep slope for 1 and 0.5 M while the degradation curve for 0.1 and 0.05 M is low sloping.1M concentration achieved more than 90% degradation in the quickest time.

Fig 4.16b shows a steeply sloping curve for 1M and 0.5 M concentration and a linear curve for 0.1 M and 0.05 M concentration. Both plots showed an increase in degradation efficiency from 0.05 M to 1M of the supporting electrolyte solution. 99.7 % and 99.9 % were the highest degradation efficiency achieved by 1 M NaCl and 1 M KCl while 28.8 % and 55.9 %2 were the lowest recorded by 0.05 M NaCl and KCl respectively. Fig 4.18 also shows that 0.5 M KCl achieved more than 90 % degradation but in lesser time (60 min) than 1 M

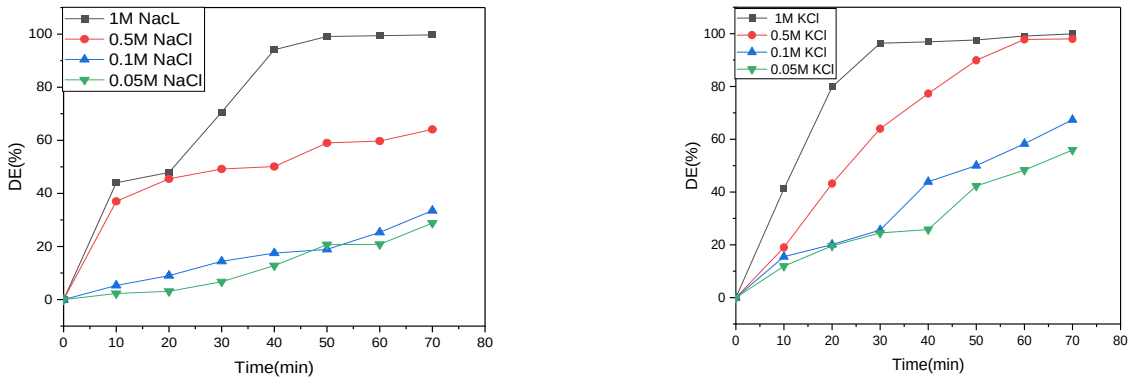


(a) (b)

**Figure 4. 16 Effect of supporting electrolyte on decolorization efficiency of BB using (a) NaCl and (b) KCl**

*(Dye concentration = 30 mg/L, Temperature (T) = 28 $^{o}$C, Voltage = 25 V, Electrolyte = 1 M KCl, Current density = 1.33 mA/mm$^{2}$, pH = 7)*

In electrocatalytic degradation, support electrolytes play a crucial role. The simulated solution is different from actual wastewater in that it is low in salt concentration and conductivity. As a result, the simulated solution has to have the right quantity of supporting electrolyte supplied. This could be attributed to an increase in the concentration and mobility of hypochlorite ions and chloride ions, which serve as the primary oxidizing species in the solution and are found in chloride salts such as KCl and NaCl. However, it is important to acknowledge that a high concentration of the supporting electrolytes could potentially adversely affect the color removal process (Zainal *et al.*, 2005). Kaur & Kaur, (2016) conducted a comparative investigation of KCl and NaCl, which further confirms that KCl serves as a superior supporting electrolyte compared to NaCl.

### 4.3.4 Effect of Temperature

The experiments were conducted at temperatures of 28°C, 38°C, 48°C, and 58°C, using a concentration of 30 mg/L, to identify the ideal temperature for degrading MG and BB solutions.The resultant effect of temperature on electrochemical degradation is shown in fig 4.17 and 4.18.The degradation profile in fig. 4.17 can be divided into 2 regions. The region of rapid linear growth (0-20 min) and a region of steady state (30-70 min). The overall trend shows an increase in degradation efficiency with time. $48^0$C achieved more than 90 % degradation in the fastest time of 30 min.

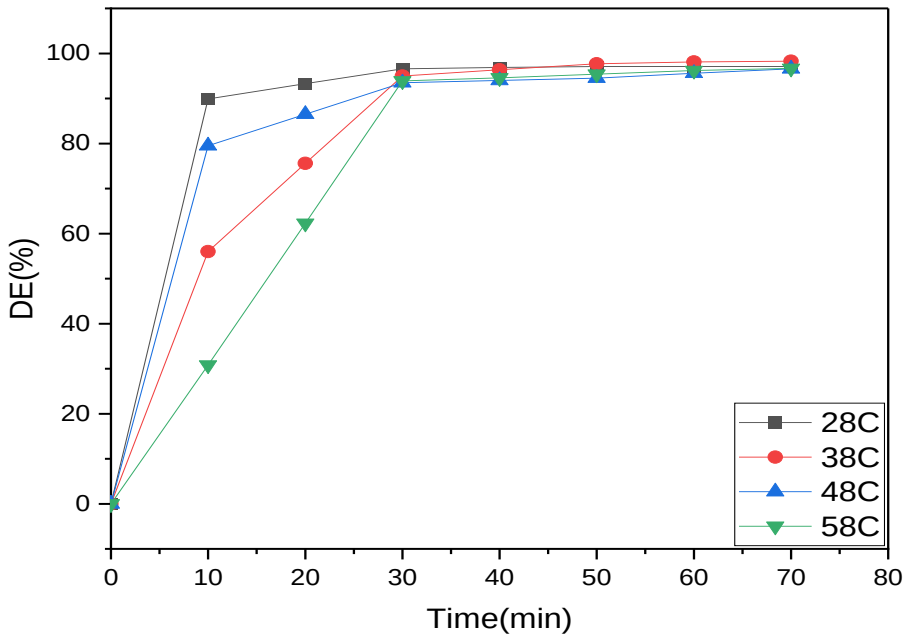


**Figure 4. 17 Decolorization of MG at Different Temperatures**

*(Dye concentration = 30mg/L, Temperature (T) = 28 °C, Voltage = 25 V, Electrolyte = 1 M KCl, Current density = 1.33mA/mm$^2$, pH = 7)*

The degradation profile in fig. 4.18 can also be divided into 2 regions. The region of rapid linear growth (0-30 min) and a region of steady state (40-70 min). The overall trend shows an increase in degradation efficiency with time. $48^0$C achieved more than 90% degradation in the fastest time of 30 min.

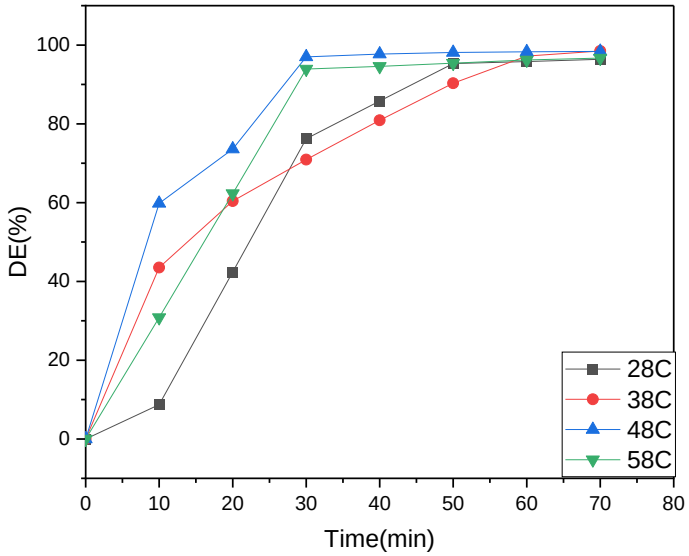


**Figure 4. 18 Decolorization of BB at Different Temperatures**

*(Dye concentration = 30mg/L, Temperature (T) = 28°C, Voltage = 25 V, Electrolyte = 1 M KCl, Current density = 1.33mA/mm$^2$)*

The impact of temperature on the electro-oxidation of organics is not consistently predictable and varies depending on the specific organic compound and the environment. While higher temperatures are generally expected to enhance reaction rates, some cases have shown that electro-oxidation and decolorization rates may decrease. For example, studies by Ma et al. (2007) demonstrated that temperatures above 25°C led to decreased rates of electro-catalytic oxidation and de-colorization of methyl orange in water containing NaCl as a supporting electrolyte. Similarly, Panizza and Cerisola (2008) observed hindered electrochemical oxidation of acid blue 22 by a boron-doped diamond electrode at higher temperatures. Rajkumar et al. (2007) found that

the ability of reactive blue 19 to be electrochemically decolored in a chloride solution was less effective as the temperature rose. These findings align with our present study.

The influence of temperature on electro-oxidation systems has dual effects. On one hand, it increases the oxidation rate of organic contaminants by oxidizing species in the solution, and on the other hand, it initiates the decomposition of the oxidizing species. It has been suggested that temperature has minimal impact on electro-oxidation processes involving OH• radicals, while the generation of chlorine/hypochlorite is hindered by an increase in temperature (Ma et al., 2007; Panizza & Cerisola, 2008).

### 4.3.5 UV-Visible Spectrum

After various times during electrolysis, typical UV-visible analysis for untreated and treated dye solutions was performed, and changes in dye solutions' absorbance were examined.

The UV-Visible spectrum of electrochemical degradation of Bromophenol Blue dye and Malachite green dye contaminated are shown in Figures 4.19 and 4.20 respectively.

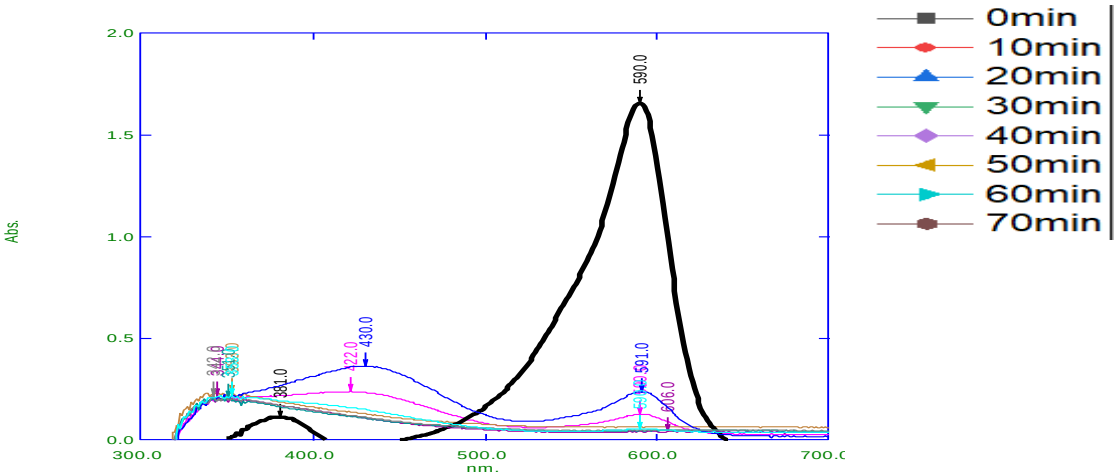


**Figure 4. 19 UV-Visible spectra of degradation of BB at different time intervals**

The plot in figure 4.19 shows the UV-VIS absorption of BB dye-contaminated water at various times during treatment. Several peaks were formed around 590 nm, 450 nm, 380 nm, and 320nm. Zero minutes achieved the highest absorbance while 70 min was the lowest at 590 nm. The plot also shows a very rapid decline in absorbance value at 590 nm between 0 min and 70 min.

At 0 minutes, the highest absorption peak strength was observed at 590 nm, corresponding to the chromophore group in the Bromophenol Blue molecule.With increasing reaction time, absorption peak intensity dropped, notably at 590 nm, suggesting that BB had experienced a considerable oxidative breakdown. The discovery of a novel absorption wavelength at 420 nm indicates the presence of a less conjugated aromatic intermediate. Additionally, the peak at 400 nm moves to a shorter wavelength. Therefore, the characteristics of BB degradation on anodes involve rapid mineralization and minimal accumulation of aromatic intermediates.

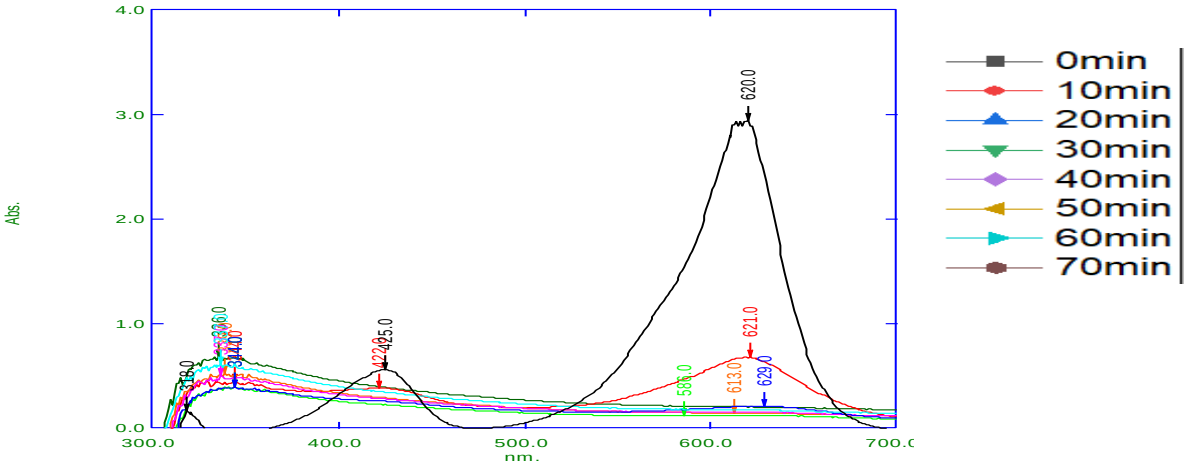


**Figure 4. 20 UV-Visible spectra of degradation of MG at different time intervals**

The plot in figure 4.20 shows the UV-VIS absorption of MG dye-contaminated water at various times during treatment. Several peaks were formed around 620 nm, 420 nm, and 320nm. Zero minutes achieved the highest absorbance while 70 min was the lowest at 590 nm. The plot also

shows a very rapid decline in absorbance value at 590 nm between 0 min and 70 min. There is also a shift in absorption at 420 nm for 0 min to 320 nm for another time.

The chromophore aromatic rings and the dye molecule's acid function are represented as absorbance peaks in the MG spectrum at 620 nm, 420 nm, and 316 nm, respectively. The rapid decline in absorbance after 0 minutes at 620 nm and the shift toward shorter wavelengths can be attributed to intermediate and aromatic ring decolorization /degradation. The absorbance at 620 nm was nearly negligible after 70 minutes of EC treatment, demonstrating the lack of auxochrome groups -N($CH_3$) in charge of the MG dye's hue. The presence of mono aromatic rings in the solution is indicated by the peak at 316 nm shifting to shorter wavelengths (209 and 185 nm) after 50 minutes of treatment. The N-demethylating process results in a change in the location of spectral peaks to shorter wavelengths, or hypsochromic shifts. This shift can also be brought on by modifications in solvatochromic factors, such as solvent polarity.

Generally, most absorption spectroscopy of organic compounds is based on transitions of n or p electrons to the p* excited state. This is because the absorption peaks for these transitions fall in an experimentally convenient region of the spectrum (200 nm – 800 nm). These transitions need an unsaturated group in the molecule to provide the p electrons. —N=N bonds and aromatic rings were broken during the electrochemical breakdown, which caused the absorbance band of the dye solutions to narrow. Additionally, the absorption band has changed from the visible to the UV area, showing that larger dye molecules have disintegrated into tiny pieces. A decline in absorbance in the visible region of the spectrum indicates the loss of a conjugated system in the chemicals. This suggests that oxidative species first oxidized dyes before converting them into carboxylic intermediates, which may ultimately result in the full mineralization of carbon into $CO_2$. Although measurements of absorbance cannot tell if full mineralization happens (Jović *et al*., 2013).

The spectrum of the absorbing species can be influenced by the solvent in which it is dissolved. When solvent polarity increases, peaks resulting from n→p* transitions shift to shorter wavelengths (blue shift). This occurs because the lone pair experiences greater salvation, which

lowers the energy of the n orbital. Conversely, p→p* transitions may sometimes show the reverse effect (i.e., redshift). This redshift is caused by attractive polarization forces between the solvent and the absorber, which lower the energy levels of both the excited and unexcited states. This effect is more pronounced for the excited state, slightly reducing the energy difference between the excited and unexcited states, leading to a small redshift. While this effect also influences n→p* transitions, it is overshadowed by the blue shift resulting from the solvation of lone pairs.

### 4.3.6 Kinetic Approach

The most convenient method to monitor the rate of dye decolorization is by observing color loss over time. The rate of the reaction can be determined by calculating the negative change in dye concentration over time ([dye]) divided by the change in time (time), as described by Equation (4.6). As the rate may vary over time, finite differences are used as an approximation. However, for the purpose of analyzing the initial rate of the reaction, a linear relationship between concentration and time can be assumed. Initial rate experiments are conducted to maintain reactant concentrations within 1% of their initial values.

$$\textbf{rate} = \frac{-\Delta[dye]}{\Delta time} = \textbf{K[dye]}^{x}\textbf{[OCl}^{-}\textbf{]}^{y} \qquad \textbf{4. 3}$$

$$\frac{d[dye]}{dt} = k[dye] \qquad \textbf{4. 4}$$

After integration we have

$$\ln\frac{[dye]}{[dye]} = kt \qquad \textbf{4. 5}$$

$$\textbf{[dye]} = [dye]\,e^{-kt} \qquad \textbf{4. 6}$$

Where [dye] is the initial concentration of dye, [dye] is the actual concentration, K is the rate constant ($min^{-1}$)

**Assessing Time Course in Relation to Integrated Rate Laws**

An initial rate study is a great way to determine the order with hypochlorite since the hypochlorite ion is not a colored species. On the ground that the dye is the colored reactant, determining the

reaction order with the dye necessitates a time course analysis. In a time-course study, the concentration of a reactant or product is compared with the integrated rate laws corresponding to reactions of different orders, as a function of time.

***Expression for First Order Reaction Rate***

The rate law for a reaction that is first-order in the reactant is:

$$\textbf{Rate} = \frac{-d[A]}{dt} \qquad \textbf{4. 7}$$

This rate law applies to one-reactant reactions, such as A→ Products.

This rate law can be applied to our reaction, which takes the form A + B→ Product

When compared to equation 1, the first order rate law in equation 4.8 yields x = 1 and y = 0 or

If $[OCl^-]^y$ remains constant and is included in k

$$\textbf{rate} = (k[OCl^-]^y)\,[dye]^x = K_{eff}[dye] \qquad \textbf{4. 8}$$

$K_{eff}$= is the effective rate constant (K[OCl-]y).

In simpler terms, the first-order rate law remains applicable, but we calculate an effective first-order rate constant, Keff, which considers the impact of hypochlorite concentration. To maintain a constant [OCl-]y, one can conduct experiments with a substantial amount of hypochlorite, ensuring minimal overall concentration change during the reaction. This situation is referred to as a pseudo-first order in the dyeing process.The integrated rate expression is as follows:

$$\ln\frac{[dye]}{[dye]_0} = -K_{eff}t \quad \textbf{OR} \qquad \textbf{4. 9}$$

$$\ln[dye] = K_{eff}t + \ln[dye]_0 \qquad \textbf{4. 10}$$

Where [dye]o is the initial concentration of dye at time zero and [dye] is the concentration at any Time, t.

***Expression for Second Order Rate of Reaction***

If x = 2 and y = 0 or $[OCl^-]^y$ is held constant in equation 4.6:

$$\textbf{Rate} = -\frac{d[dye]}{dt} = \mathbf{K_{eff}[dye]^2} \qquad \textbf{4. 11}$$

The reaction is pseudo-second-order in CV and integration of equation 4.12 gives

$$\frac{1}{[dye]} - \frac{1}{[dye]_0} = \mathbf{K_{eff}t} \qquad \textbf{4. 12}$$

***Determining the Order of Reaction***

As absorbance is directly proportional to concentration, following Beer's Law (A = εlc), absorbance can be used instead of concentrations for curve fitting. In a first-order reaction, the absorption coefficient cancels out in both the numerator and denominator of the ln term in Equation 4.14. Therefore, either concentration or absorbance can be utilized to directly calculate the rate constant.For a second-order reaction, since

$$\textbf{[dye] = A/el,} \qquad \textbf{4. 13}$$

$$\frac{1}{A} - \frac{1}{A0} = \frac{Keff}{\in l}\mathbf{t} \qquad \textbf{4. 14}$$

Where Ao is the starting absorbance.

Absorbance versus time measurements is collected and plotted to determine the order of a reaction. The concentration of absorbance versus the time plot for a zero-order reaction is a straight line. A plot of ln [dye] or ln A versus t for a first-order reaction should yield a straight line with a slope of $k_{eff}$, according to equation 4.12.

A plot of 1/[dye] or 1/A versus t for a second-order reaction is a straight line, according to equations 4.13 and 4.14.

To attempt to match the present data with a kinetic first-order rate equation, a graph is drawn between ln A and time t. Figures 4.21 demonstrate that BB followed a first-order reaction equation. This is similar to the result reported by Zhang et al., (2019)

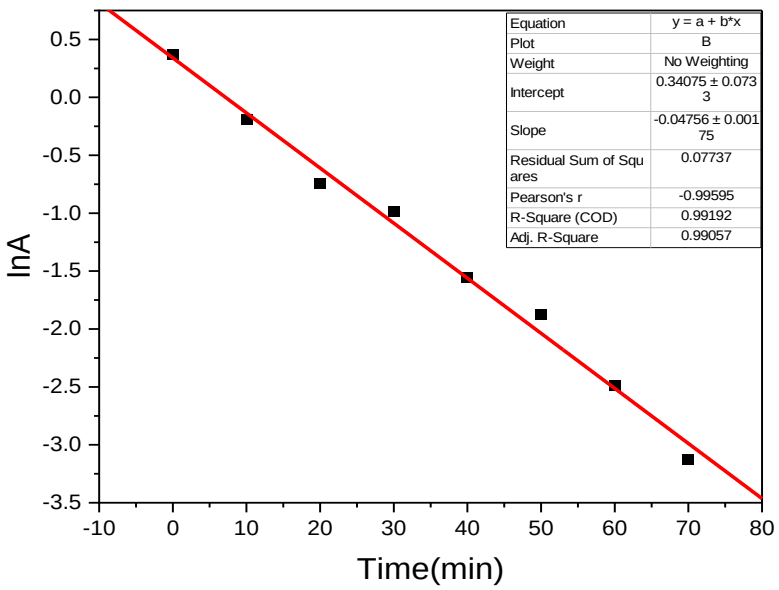


**Figure 4. 21 Kinetic studies of the first-order BB reaction at different times during electrochemical dye degradation**

The second-order equation's kinetics is then applied to the degradation data of MG. Fig.4.22 demonstrates that MG degradation obeyed the second-order kinetics. The kinetics of malachite Green degradation varies as different authors have reported different reaction orders. Chen *et al*., (2020) reported the kinetics to be first order while Kusuma *et al*., (2016)reported the kinetics to be first-order and half.

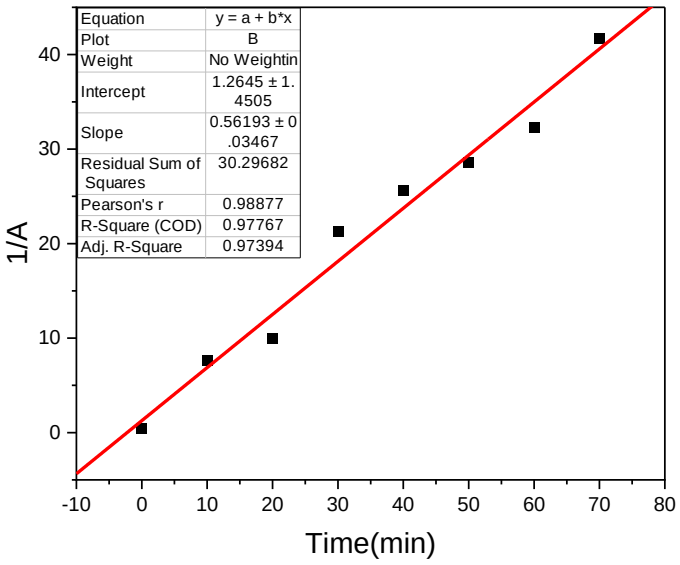


**Figure 4. 22 Kinetic studies of the second-order MG reaction at different time points during electrochemical dye degradation.**

### 4.3.7 Considering energy usage

The electrical energy consumption associated with the electrochemical degradation of BB and MG can be evaluated by measuring the amount of electrical energy (kWh) utilized during the process (Jović *et al*., 2013; Moura *et al*., 2016):

$$\boldsymbol{E(KWh)} = \frac{\boldsymbol{P(W)\,x\,t(h)}}{\boldsymbol{V_{sol}(dm^3)}} \qquad \textbf{4. 15}$$

where:

**P (W) = I (A) x v (V)** **4. 16**

P is the electrochemical cell's electrical output (measured in Watts), t is the electrolysis's time (measured in hours), V is the amount of dye solution electrolyzed (measured in dm3), I is the current (measured in Amperes), and v is voltage (in Volts).

The energy consumption figures in Table 4.2 make it possible to calculate how much energy is used to treat each cubic meter of water that has been contaminated by MG and BB to Nigeria's average power rate, which is around 60.16 NGN/kWh. This corresponds to 3510.3 NGN – 17551.7 NGN for the current range studied.

**Table 0.1 The Correlation between Applied Current and Electrical Energy Consumption during the Degradation of MG and BB at 25 V."**

| Current (A) | Voltage (V) | Time (h) | Energy Consumption ($KWh/m^3$) |
|---|---|---|---|
| 1 | 25 | 1.167 | 58.35 |
| 2 | 25 | 1.167 | 116.7 |
| 3 | 25 | 1.167 | 175.05 |
| 4 | 25 | 1.167 | 233.4 |
| 5 | 25 | 1.167 | 291.75 |

As expected, the electrical energy consumed by the process increased steadily with increasing current and is of similar magnitude as the values for electrochemical decoloration of dispersed blue 1 dye, as reviewed by (Oguzie *et al*., 2021).

### 4.3.8 DFT Computation

To theoretically understand the mechanism behind the decolorization of Bromophenol Blue and Malachite Green dyes, DFT computations were conducted. These computations involved modeling the local reactivity of the Bromophenol Blue and Malachite Green molecules to identify the active sites where the oxidative attack would commence. The computations utilized various techniques, including the Hirshfeld population analysis (Delley, 1990, 2000), the Perdew-Wang (PW) local correlation, limited spin polarization on the DND basis set, and the DMol3 software (Materials Studio).The COMPASS force field and the Smart reduction approach were used to geometrically optimize the BB molecule structure before the calculations utilizing high-convergence criteria. The optimal structure, orbital density, highest occupied molecular orbital

(HOMO), lowest unoccupied molecular orbital (LUMO), and Fukui functions of BB and MG are shown in Table 4.3

**Table 4. 2 Electronic properties of Bromophenolblue and Malachite green dye**

| | Optimized Structure | HOMO | LUMO | F+ | F- |
|---|---|---|---|---|---|
| **BB** | 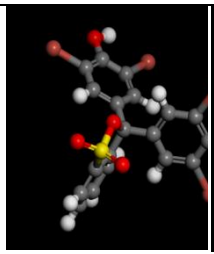 | 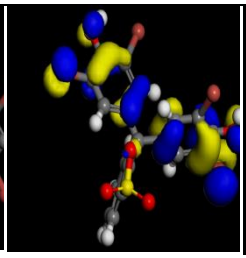 | 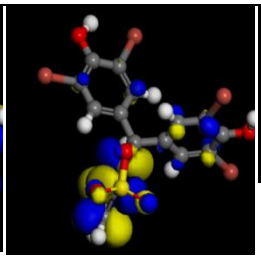 | 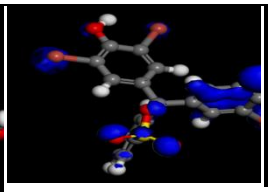 | 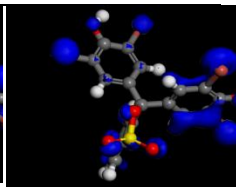 |
| **MG** | 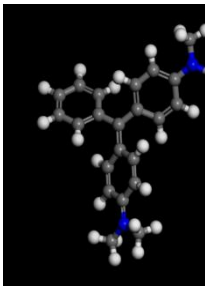 | 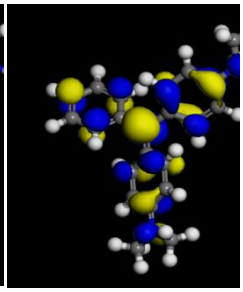 | 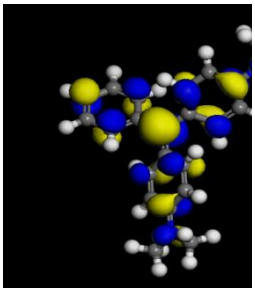 | 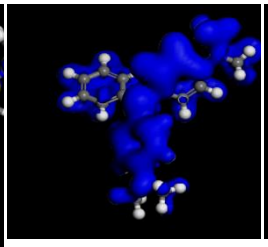 | 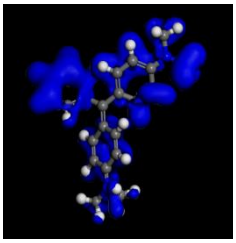 |

The HOMO regions, representing the sites most susceptible to attack by electron-seeking species, align with the electrophilic Fukui functions, which indicate the molecule's ability to donate electrons. Conversely, the LUMO regions correspond with the F+ regions, which indicate the molecule's tendency to receive electrons. By applying the theoretical principles of the hard and soft acids and bases (HSAB), it becomes feasible to elucidate the electronic structures using fundamental molecular reactivity indicators (Cerda-Monje *et al*., 2014).

As a result, the molecular and electronic structure of MG and BB are described in Tables 4.2 and 4.3 using certain quantum-chemical terms. The propensity of a species to emit electrons is indicated by a high value of HOMO. The energy required to evict an electron from the outermost orbital also decreases with the magnitude of E = LUMO - HOMO. Chemical hardness (or softness),

which promotes intimate contact between the interacting species, may be a significant determinant of the likelihood of electrophile/nucleophile interaction

**Table 0.2 features of BB's quantum chemistry as calculated**

| Chemical Parameters | Values (eV) |
|---|---|
| $E_{HOMO}$ | -6.493 |
| $E_{LUMO}$ | -2.925 |
| Energy gap, $\Delta E_{gap} = (E_{lUMO} - E_{HOMO})$ | 3.568 |
| Electrochemical potential, $\mu = -X$ | -4.709 |
| Ionization potential, I | 6.493 |
| Electron affinity, A | 2.925 |
| Electronegativity, X = (I+A)/2 | 4.709 |
| Chemical Hardness, $\eta = (I-A)/2$ | 1.784 |
| Chemical softness, $S = 1/\eta$ | 0.561 |
| Electrophilicity, $\omega = \mu^2/2\eta$ | 6.214 |
| $\Delta E$ Back donation $(-\eta/4)$ | -0.446 |

**Table 0.3 features of the MG's quantum chemistry, as calculated**

| Chemical Parameters | Values (eV) |
|---|---|
| $E_{HOMO}$ | -3.186 |
| $E_{LUMO}$ | -2.880 |
| Energy gap, $\Delta E_{gap} = (E_{lUMO} - E_{HOMO})$ | 0.306 |
| Electrochemical potential, $\mu = -X$ | -3.033 |
| Ionization potential, I | 3.186 |
| Electron affinity, A | 2.880 |
| Electronegativity, X = (I+A)/2 | 3.033 |
| Chemical Hardness, $\eta = (I-A)/2$ | 0.153 |
| Chemical softness, $S = 1/\eta$ | 6.534 |

| | |
|---|---|
| Electrophilicity,$\omega = \mu^2/2\ \eta$ | 30.062 |
| $\Delta$E Back donation ($-\eta/4$) | -0.038 |

BromophenolBlue molecules' reactive areas were evaluated using the Fukui indices (FI) for nucleophilic (F+), electrophilic (F-), and radical (F0) attacks. In Table 4.4, the derived Fukui functions BB are displayed.

**Table 0.4 values of the radical, nucleophilic, and electrophilic Fukui indices for BB**

| **No/ Atom** | **$F^-$** | **$F^+$** | **$F^0$** |
|---|---|---|---|
| C (1) | 0.027 | 0.014 | 0.021 |
| C (2) | 0.016 | -0.000 | 0.008 |
| C (3) | 0.028 | -0.007 | 0.010 |
| C (4) | 0.019 | 0.010 | 0.014 |
| C (5) | 0.016 | 0.011 | 0.014 |
| C (6) | 0.033 | 0.013 | 0.023 |
| C (7) | 0.002 | 0.002 | 0.002 |
| C (8) | 0.030 | -0.004 | 0.013 |
| C (9) | -0.009 | 0.029 | 0.010 |
| C (10) | 0.028 | 0.016 | 0.022 |
| C (11) | 0.015 | 0.018 | 0.016 |
| C (12) | 0.035 | 0.014 | 0.025 |
| C (13) | 0.035 | 0.016 | 0.025 |
| C (14) | 0.016 | 0.001 | 0.008 |
| C (15) | -0.004 | 0.050 | 0.023 |
| C (16) | 0.010 | 0.087 | 0.049 |
| C (17) | 0.016 | 0.087 | 0.030 |

| | | | |
|---|---|---|---|
| C (18) | 0.012 | 0.067 | 0.040 |
| C (19) | 0.002 | 0.060 | 0.031 |
| Br (20) | 0.062 | 0.043 | 0.052 |
| Br (21) | 0.125 | 0.050 | 0.087 |
| Br (22) | 0.066 | 0.059 | 0.062 |
| Br (23) | 0.150 | 0.053 | 0.101 |
| O (24) | 0.053 | 0.020 | 0.036 |
| O (25) | 0.055 | 0.020 | 0.038 |
| H (26) | 0.019 | 0.010 | 0.014 |
| H (27) | 0.020 | 0.011 | 0.015 |
| S (28) | 0.006 | 0.027 | 0.017 |
| O (29) | 0.022 | 0.046 | 0.034 |
| O (30) | 0.011 | 0.045 | 0.028 |
| O (31) | 0.002 | 0.018 | 0.010 |
| H (32) | 0.014 | 0.001 | 0.007 |
| H (33) | 0.008 | 0.001 | 0.007 |
| H (34) | 0.015 | 0.011 | 0.013 |
| H (35) | 0.013 | 0.001 | 0.007 |
| H (36) | -0.001 | 0.029 | 0.014 |
| H (37) | 0.010 | 0.044 | 0.027 |
| H (38) | 0.013 | 0.031 | 0.022 |
| H (39) | 0.011 | 0.036 | 0.024 |

The information in Table 4.4 indicates that the different functional groups in the BB molecule are more reactive to electrophilic attack in the following order: Br23*>Br21>Br20>Br22 >O25>O24>C12=C13>C8>C10>O29>S28.* This indicates that the bromine atom in the 3,5-dibromo-4-hydroxyphenyl group is the most vulnerable to assault by oxidizing (electrophilic) species. The reactivity order for the nucleophilic attack, which corresponds to *C17=C16>C18>C19>Br22>Br23>Br21=C15>O29>O30>Br20>S28>O24* shows the most reactive sites to be on the Benzoxathiole group. Both attacks appear to be equally likely based on

the nucleophilic and electrophilic reactivity index values.The radical reactivity order; Br23>Br21>Br22>Br20>C16>C18>C19>O25>O24>O29>C17>O30>S28>O31 suggests the possibility of attack mainly on the 3,5-dibromo-4-hydroxyphenyl group moiety. The results of the computed quantum chemical descriptors indicate that the main reactive sites responsible for the oxidative decolorization of BB are situated on the Bromine atom within the 3,5-dibromo-4-hydroxyphenyl group.This finding is in line with the study conducted by (Cong *et al*., 2021) Malachite Green dye molecules' reactive areas were also evaluated using the Fukui indices (FI) for nucleophilic ($F^+$), electrophilic ($F^-$), and radical ($F^0$) attacks. In Table 4.5, the derived Fukui functions BB are displayed.

**Table 0.5 calculated values for the MG's radical, nucleophilic, and electrophilic Fukui indices**

| No/Atom | $F^-$ | $F^+$ | $F^0$ |
|---|---|---|---|
| C (1) | 0.049 | 0.053 | 0.051 |
| C (2) | 0.026 | 0.028 | 0.027 |
| C (3) | 0.025 | 0.027 | 0.026 |
| C (4) | 0.008 | 0.010 | 0.009 |
| C (5) | 0.025 | 0.027 | 0.026 |
| C (6) | 0.026 | 0.028 | 0.027 |
| C (7) | 0.071 | 0.083 | 0.077 |
| C (8) | 0.010 | 0.007 | 0.008 |
| C (9) | 0.009 | 0.006 | 0.007 |
| C (10) | 0.025 | 0.024 | 0.025 |
| C (11) | 0.024 | 0.023 | 0.023 |
| C (12) | 0.032 | 0.033 | 0.032 |
| C (13) | 0.023 | 0.022 | 0.023 |
| C (14) | 0.024 | 0.025 | 0.024 |
| C (15) | 0.024 | 0.023 | 0.023 |
| C (16) | 0.023 | 0.022 | 0.023 |
| C (17) | 0.031 | 0.032 | 0.031 |

| | | | |
|---|---|---|---|
| C (18) | 0.023 | 0.022 | 0.023 |
| C (19) | 0.023 | 0.024 | 0.024 |
| N (20) | 0.032 | 0.028 | 0.030 |
| N (21) | 0.031 | 0.027 | 0.029 |
| C (22) | 0.011 | 0.010 | 0.010 |
| C (23) | 0.011 | 0.010 | 0.010 |
| C (24) | 0.010 | 0.010 | 0.010 |
| C (25) | 0.010 | 0.010 | 0.010 |
| H (26) | 0.027 | 0.029 | 0.028 |
| H (27) | 0.021 | 0.022 | 0.021 |
| H (28) | 0.012 | 0.013 | 0.013 |
| H (29) | 0.012 | 0.013 | 0.013 |
| H (30) | 0.021 | 0.022 | 0.021 |
| H (31) | 0.013 | 0.013 | 0.013 |
| H (32) | 0.017 | 0.017 | 0.017 |
| H (33) | 0.017 | 0.017 | 0.017 |
| H (34) | 0.012 | 0.012 | 0.012 |
| H (35) | 0.013 | 0.012 | 0.012 |
| H (36) | 0.017 | 0.017 | 0.017 |
| H (37) | 0.017 | 0.017 | 0.017 |
| H (38) | 0.012 | 0.012 | 0.012 |
| H (39) | 0.016 | 0.015 | 0.015 |
| H (40) | 0.015 | 0.014 | 0.014 |
| H (41) | 0.016 | 0.015 | 0.015 |
| H (42) | 0.016 | 0.015 | 0.016 |
| H (43) | 0.014 | 0.013 | 0.013 |
| H (44) | 0.016 | 0.015 | 0.015 |
| H (45) | 0.015 | 0.015 | 0.015 |

| | | | |
|---|---|---|---|
| H (46) | 0.015 | 0.014 | 0.015 |
| H (47) | 0.014 | 0.013 | 0.014 |
| H (48) | 0.015 | 0.014 | 0.014 |
| H (49) | 0.015 | 0.015 | 0.015 |
| H (50) | 0.015 | 0.014 | 0.014 |

According to the information in Table 4.5, the different functional groups in the MG molecule should be attacked by electrophiles in the following order: C7*>C1>C12=N20>C17=N21 >C2=C6>C10=C3.* This means that the most reactive site for attack by oxidizing (electrophilic) species is the phenyl methylene group. The reactivity order for the nucleophilic attack, which corresponds to *C7>C1>C12>C17>C6=C2=N20>C3=C5=N21>C14 s*hows the most reactive sites to be also in the Phenyl methylene group. The radical reactivity order; C7>C1>C17>N20>N21>C2=C6 also suggests the same possibility. The nucleophilic, electrophilic, and radical reactivity indices' values indicate that all types of attacks are equally likely. Additionally, the computed quantum chemical descriptors show that the primary reactive sites responsible for the oxidative decolorization of MG are situated on the carbon atom within the methylene group.The work of (Singh *et al*., 2013; Sasidharan Pillai & Gupta, 2016) provides evidence for this

# CHAPTER FIVE

# CONCLUSION AND RECOMMENDATION

## **5.1** Conclusion

Based on findings from this research it can be concluded that Bromophenol Blue (BB) dye and Malachite Green (MG) dye contaminated can be degraded to high efficiency with the electrochemical method. Operating variables including temperature, PH, current density, and supporting electrolyte type had minimal impact on the degradation efficiency, whereas supporting electrolyte concentration showed a more marked shift. Generally, it was observed that the highest degradation efficiency occurred in acidic media, high current density, high electrolyte concentration, and temperature range of $38^0$C to $48^0$C. DFT calculations indicate oxidative attack to be initiated at the Bromine atom of the hydro-phenyl group for BB and Carbon of the methylene group for MG.

Bacteria and fungi strains were successfully isolated and cultured from MG and BB dye-polluted soil respectively. High degradation efficiency was recorded for MG but not for BB. Bioelectricity was successfully produced from MG and BB dye-contaminated water. BB dye-contaminated water achieves the highest power density.

## **5.2** Contribution To Knowledge

With its two-prong approach, this work has significantly added to the database of coupled systems for efficient treatment of dye-contaminated water and simultaneous electricity production. This will greatly assist wastewater water treatment managers and environmentalists to make better cost-effective and energy-efficient decisions about wastewater treatment.

## **5.2 Recommendation**

1) Further studies should be carried out to determine the biodegradation mechanism of BB and MG by the isolated strains.

2) A continuous-reactor MFC design for both BB and MG dye-contaminated water should be studied to better understand the current producing capacity of the dyes.
3) COD, TOC, and other water treatment analyses should be carried out in both the microbial degradation and MFC to determine the extent of re-useability of the wastewater.

# REFERENCE


Abdi, J., Vossoughi, M., Mahmoodi, N. M., & Alemzadeh, I. (2017). Synthesis of metal-organic framework hybrid nanocomposites based on GO and CNT with high adsorption capacity for dye removal. *Chemical Engineering Journal*, *326*, 1145–1158. https://doi.org/10.1016/j.cej.2017.06.054

Adegoke, K. A., & Bello, O. S. (2015). Dye sequestration using agricultural wastes as adsorbents. *Water Resources and Industry*, *12*, 8–24. https://doi.org/10.1016/j.wri.2015.09.002

Adeleye, S., & Okorondu, S. (2015). Bioelectricity from students' hostel waste water using microbial fuel cell. *International Journal of Biological and Chemical Sciences*, *9*(2), 1038. https://doi.org/10.4314/ijbcs.v9i2.39

Ali, H. (2010). Biodegradation of synthetic dyes - A review. *Water, Air, and Soil Pollution*, *213*(1–4), 251–273. https://doi.org/10.1007/s11270-010-0382-4

ANAND, S. V., & MISRA, M. (2017). Decolourization of industrial dyes using Ascomycetes and mucor species. *International Journal of Pharma and Bio Sciences*, *8*(2). https://doi.org/10.22376/IJPBS.2017.8.2.B285-291

Ansari, A., & Nematollahi, D. (2018). A comprehensive study on the electrocatalytic degradation, electrochemical behavior and degradation mechanism of malachite green using electrodeposited nanostructured B-PbO2 electrodes. *Water Research*, *144*, 462–473. https://doi.org/10.1016/j.watres.2018.07.056

Anuforo, H. U., Ogbulie, T. E., Akujobi, C. O., & Ezeji, E. U. (2017). Study on the use of microbial fuel cell as waste management option to generate electricity from piggery wastewater. *Analele Universitatii Din Oradea, Fascicula Biologie*, *24*(1), 40–47.

Aquino Neto, S., & de Andrade, A. R. (2009). Electrooxidation of glyphosate herbicide at different DSA® compositions: pH, concentration and supporting electrolyte effect. *Electrochimica Acta*, *54*(7), 2039–2045. https://doi.org/10.1016/j.electacta.2008.07.019

Baddouh, A. A., Bessegato, G. G., Hilali, M., Valnice, M., & Zanoni, B. (2018). PT. *Biochemical Pharmacology*. https://doi.org/10.1016/j.jece.2018.03.007

Bae, J. S., & Freeman, H. S. (2007). Aquatic toxicity evaluation of copper-complexed direct dyes to the Daphnia magna. *Dyes and Pigments*, *73*(1), 126–132. https://doi.org/10.1016/j.dyepig.2005.10.019

Banerjee, U. C. (2007). *Technology Removal of Dyes from the Effluent of Textile and Dyestuff Manufacturing Industry : A Review of Emerging Techniques With Reference to Biological Treatment Removal of Dyes from the Effluent of Textile and Dyestuff Manufacturing Industry : A Revie*. *3389*. https://doi.org/10.1080/10643380590917932

Bayoumi, M. N., Al-wasify, R. S., & Hamed, S. R. (2014). Bioremediation of Textile Wastewater Dyes using Local Bacterial Isolates. *International Journal of Current Miccrobiology and Applied Science*, *3*(12), 962–970.

Cerda-Monje, A., Ormazábal-Toledo, R., Cárdenas, C., Fuentealba, P., & Contreras, R. (2014). Regional electrophilic and nucleophilic Fukui functions efficiently highlight the lewis acidic/basic regions in ionic liquids. *Journal of Physical Chemistry B*, *118*(13), 3696–3701. https://doi.org/10.1021/jp5009994

Chacko, J. T., & Subramaniam, K. (2011). Enzymatic Degradation of Azo Dyes – A Review. *International Journal Of Environmetal Sciences*, *1*(6), 1250–1260. https://doi.org/10.6088/ijes.00106020018

Chander, M., & Arora, D. S. (2007). Evaluation of some white-rot fungi for their potential to decolourise industrial dyes. *Dyes and Pigments*, *72*(2), 192–198. https://doi.org/10.1016/j.dyepig.2005.08.023

Cheesbrough, M. (2004). *District Laboratory Practice in Tropical Countries 1* (Second). Cambridge University Press.

Chen, Y., Fan, D., Huang, L., Li, Y., Qiu, Z., & Feng, C. (2020). Efficient Electrochemical Degradation of Malachite Green Using Fluorine Doped Tin Oxide (FTO) Conductive Glass as Anode. *International Journal of Electrochemical Science*, *15*(11), 11437–11453. https://doi.org/10.20964/2020.11.12

Christie, R. (2007). *Environmental Aspect of Textile Dyeing*. WoodHead Publishing in Textile.

Cong, Q., Ren, M., Zhang, T., Cheng, F., & Qu, J. (2021). Efficient photoelectrocatalytic performance of beta-cyclodextrin/graphene composite and effect of Cl−in water: degradation for bromophenol blue as a case study. *RSC Advances*, *11*(48), 29896–29905. https://doi.org/10.1039/d1ra04533d

Crini, G. (2006). Non-conventional low-cost adsorbents for dye removal: A review. *Bioresource Technology*, *97*(9), 1061–1085. https://doi.org/10.1016/j.biortech.2005.05.001

Dai, Q., Shen, H., Xia, Y., Chen, F., Wang, J., & Chen, J. (2013). The application of a novel Ti/SnO2-Sb2O 3/PTFE-La-Ce-β-PbO2 anode on the degradation of cationic gold yellow X-GL in sono-electrochemical oxidation system. *Separation and Purification Technology*, *104*, 9–16. https://doi.org/10.1016/j.seppur.2012.10.043

Dai, Q., Zhou, J., Weng, M., Luo, X., Feng, D., & Chen, J. (2016). Electrochemical oxidation metronidazole with Co modified PbO2 electrode: Degradation and mechanism. *Separation and Purification Technology*, *166*, 109–116. https://doi.org/10.1016/j.seppur.2016.04.028

De Gisi, S., Lofrano, G., Grassi, M., & Notarnicola, M. (2016). Characteristics and adsorption capacities of low-cost sorbents for wastewater treatment: A review. *Sustainable Materials and Technologies*, *9*, 10–40. https://doi.org/10.1016/j.susmat.2016.06.002

Duan, X., Ma, F., Yuan, Z., Jin, X., & Chang, L. (2013). Electrochemical degradation of phenol in aqueous solution using PbO2 anode. *Journal of the Taiwan Institute of Chemical Engineers*, *44*(1), 95–102. https://doi.org/10.1016/j.jtice.2012.08.009

El-Gohary, F., & Tawfik, A. (2009). Decolorization and COD reduction of disperse and reactive dyes wastewater using chemical-coagulation followed by sequential batch reactor (SBR) process. *Desalination*, *249*(3), 1159–1164. https://doi.org/10.1016/j.desal.2009.05.010

Fu, Y., & Viraraghavan, T. (2001). Fungal decolorization of dye wastewaters: A review. *Bioresource*

*Technology*, *79*(3), 251–262. https://doi.org/10.1016/S0960-8524(01)00028-1

Gupta, V. K. (2009). Application of low-cost adsorbents for dye removal – A review. *Journal of Environmental Management*, *90*(8), 2313–2342. https://doi.org/10.1016/j.jenvman.2008.11.017

Gupta, V. K., Carrott, P. J. M., Ribeiro Carrott, M. M. L., & Suhas. (2009). Low-Cost adsorbents: Growing approach to wastewater treatmenta review. *Critical Reviews in Environmental Science and Technology*, *39*(10), 783–842. https://doi.org/10.1080/10643380801977610

Harsini, M., Fitria, F., & Pudjiastuti, P. (2016). *Electrochemical Degradation of Malachite Green using Nanoporous Carbon Paste Electrode*. *070002*. https://doi.org/10.1063/1.4943332

Hou, B., Sun, J., & Hu, Y. (2011). Effect of enrichment procedures on performance and microbial diversity of microbial fuel cell for Congo red decolorization and electricity generation. *Applied Microbiology and Biotechnology*, *90*(4), 1563–1572. https://doi.org/10.1007/s00253-011-3226-2

Joshi, B., Kabariya, K., Nakrani, S., Khan, A., M. Parabia, F., V. Doshi, H., & Chandra Thakur, M. (2013). Biodegradation of Turquoise Blue Dye by Bacillus Megaterium Isolated from Industrial Effluent. *American Journal of Environmental Protection*, *1*(2), 41–46. https://doi.org/10.12691/env-1-2-5

Jović, M., Stanković, D., Manojlović, D., Andelković, I., Milić, A., Dojćinović, B., & Roglić, G. (2013). Study of the electrochemical oxidation of reactive textile dyes using platinum electrode. *International Journal of Electrochemical Science*, *8*(1), 168–183.

Kalathil, S., Lee, J., & Cho, M. H. (2011). Granular activated carbon based microbial fuel cell for simultaneous decolorization of real dye wastewater and electricity generation. *New Biotechnology*, *29*(1), 32–37. https://doi.org/10.1016/j.nbt.2011.04.014

Kalathil, S., Lee, J., & Cho, M. H. (2012). Efficient decolorization of real dye wastewater and bioelectricity generation using a novel single chamber biocathode-microbial fuel cell. *Bioresource Technology*, *119*, 22–27. https://doi.org/10.1016/j.biortech.2012.05.059

Kang, Y., Xu, X., Pan, H., Tian, J., Tang, W., & Liu, S. (2018). Decolorization of mordant yellow 1 using aspergillus sp. Ts-a cgmcc 12964 by biosorption and biodegradation. *Bioengineered*, *9*(1), 222–232. https://doi.org/10.1080/21655979.2018.1472465

Kariyajjanavar, P., Jogttappa, N., & Nayaka, Y. A. (2011). Studies on degradation of reactive textile dyes solution by electrochemical method. *Journal of Hazardous Materials*, *190*(1–3), 952–961. https://doi.org/10.1016/j.jhazmat.2011.04.032

Katheresan, V., Kansedo, J., & Lau, S. Y. (2018). Efficiency of various recent wastewater dye removal methods: A review. *Journal of Environmental Chemical Engineering*, *6*(4), 4676–4697. https://doi.org/10.1016/j.jece.2018.06.060

Kaur, R., & Kaur, H. (2016). Electrochemical degradation of Congo red from aqueous solution: Role of graphite anode as electrode material. *Portugaliae Electrochimica Acta*, *34*(3), 185–196. https://doi.org/10.4152/pea.201603185

Kaushik, P., & Malik, A. (2009). Fungal dye decolourization: Recent advances and future potential.

*Environment International*, *35*(1), 127–141. https://doi.org/10.1016/j.envint.2008.05.010

Kumar, A., Chopra, J., Singh, S. K., Khan, A., & Singh, R. N. (2015). Biodegradation of azo dyes by Bacillus subtilis "RA29." *Der Pharmacia Lettre*, *7*(6), 234–238.

Kumar, S. S., Kumar, V., Kumar, R., Malyan, S. K., & Pugazhendhi, A. (2019). Microbial fuel cells as a sustainable platform technology for bioenergy, biosensing, environmental monitoring, and other low power device applications. *Fuel*, *255*. https://doi.org/10.1016/j.fuel.2019.115682

Kumar, S. S., Kumar, V., Malyan, S. K., Sharma, J., Mathimani, T., Maskarenj, M. S., Ghosh, P. C., & Pugazhendhi, A. (2019). Microbial fuel cells (MFCs) for bioelectrochemical treatment of different wastewater streams. *Fuel*, *254*. https://doi.org/10.1016/j.fuel.2019.05.109

Kusuma, H. S., Sholihuddin, R. I., Harsini, M., & Darmokoesoemo, H. (2016). Electrochemical degradation of malachite green dye using carbon/Tio2 electrodes. *Journal of Materials and Environmental Science*, *7*(4), 1454–1460.

Li, Z., Zhang, X., Lin, J., Han, S., & Lei, L. (2010). Azo dye treatment with simultaneous electricity production in an anaerobic-aerobic sequential reactor and microbial fuel cell coupled system. *Bioresource Technology*, *101*(12), 4440–4445. https://doi.org/10.1016/j.biortech.2010.01.114

Liu, H., Ramnarayanan, R., & Logan, B. E. (2004). Production of Electricity during Wastewater Treatment Using a Single Chamber Microbial Fuel Cell. *Environmental Science and Technology*, *38*(7), 2281–2285. https://doi.org/10.1021/es034923g

Liu, L., Li, F. B., Feng, C. H., & Li, X. Z. (2009). Microbial fuel cell with an azo-dye-feeding cathode. *Applied Microbiology and Biotechnology*, *85*(1), 175–183. https://doi.org/10.1007/s00253-009-2147-9

Lu, X., Yang, B., Chen, J., & Sun, R. (2009). Treatment of wastewater containing azo dye reactive brilliant red X-3B using sequential ozonation and upflow biological aerated filter process. *Journal of Hazardous Materials*, *161*(1), 241–245. https://doi.org/10.1016/j.jhazmat.2008.03.077

Ma, H., Wang, B., & Luo, X. (2007). Studies on degradation of Methyl Orange wastewater by combined electrochemical process. *Journal of Hazardous Materials*, *149*(2), 492–498. https://doi.org/10.1016/j.jhazmat.2007.04.020

Makarem, M. A. (2018). *The Role and Application of Nanomaterials in the Process of Water Purification (in Persian)*. *July*.

Maleki, A., Hamesadeghi, U., Daraei, H., Hayati, B., Najafi, F., McKay, G., & Rezaee, R. (2017). Amine functionalized multi-walled carbon nanotubes: Single and binary systems for high capacity dye removal. *Chemical Engineering Journal*, *313*, 826–835. https://doi.org/10.1016/j.cej.2016.10.058

Masindi, V., & Muedi, K. L. (2018). Environmental Contamination by Heavy Metals. *Heavy Metals*. https://doi.org/10.5772/intechopen.76082

Miao, D., Liu, G., Wei, Q., Hu, N., Zheng, K., Zhu, C., Liu, T., Zhou, K., Yu, Z., & Ma, L. (2020). Electro-activated persulfate oxidation of malachite green by boron-doped diamond (BDD) anode: Effect of degradation process parameters. *Water Science and Technology*, *81*(5), 925–935.

https://doi.org/10.2166/wst.2020.176

Mohanakrishna, G., Al-Raoush, R. I., & Abu-Reesh, I. M. (2021). Integrating electrochemical and bioelectrochemical systems for energetically sustainable treatment of produced water. *Fuel*, *285*. https://doi.org/10.1016/j.fuel.2020.119104

Mojsov, K. D., Andronikov, D., Janevski, A., Kuzelov, A., & Gaber, S. (2016). The Application of Enzymes for the Removal of Dyes From. *Advanced Technologies*, *5*(1), 81–86.

Moura, D. C. De, Quiroz, M. A., Silva, D. R. Da, Salazar, R., & Martínez-Huitle, C. A. (2016). Electrochemical degradation of Acid Blue 113 dye using TiO2-nanotubes decorated with PbO2 as anode. *Environmental Nanotechnology, Monitoring and Management*, *5*, 13–20. https://doi.org/10.1016/j.enmm.2015.11.001

Nakamura, K. C., Guimarães, L. S., Magdalena, A. G., Angelo, A. C. D., De Andrade, A. R., Garcia-Segura, S., & Pipi, A. R. F. (2019). Electrochemically-driven mineralization of Reactive Blue 4 cotton dye: On the role of in situ generated oxidants. *Journal of Electroanalytical Chemistry*, *840*(March), 415–422. https://doi.org/10.1016/j.jelechem.2019.04.016

Nguyen, T. A., & Juang, R. S. (2013). Treatment of waters and wastewaters containing sulfur dyes: A review. *Chemical Engineering Journal*, *219*, 109–117. https://doi.org/10.1016/j.cej.2012.12.102

Ning, X. A., Yang, C., Wang, Y., Yang, Z., Wang, J., & Li, R. (2014). Decolorization and biodegradation of the azo dye Congo red by an isolated Acinetobacter baumannii YNWH 226. *Biotechnology and Bioprocess Engineering*, *19*(4), 687–695. https://doi.org/10.1007/s12257-013-0729-y

Oguzie, K., Oguzie, E., Nwanonenyi, S., Edoziem, J., & Vrsalović, L. (2021). Electrochemical decolorization of Disperse Blue-1 dye in aqueous solution. *Environmental Engineering and Management Journal*, *20*(9), 1467–1476. https://doi.org/10.30638/eemj.2021.136

Olumide D. Olukanni, Aliu Adenopo, Ayodeji O. Awotula, & Akinniyi A. Osuntoki. (2021). Biodegradation of Malachite Green by Extracellular Laccase Producing Bacillus thuringiensis RUN1. *Journal of Basic & Applied Sciences*, *9*, 543–549. https://doi.org/10.6000/1927-5129.2013.09.70

Panizza, M., & Cerisola, G. (2008). Removal of colour and COD from wastewater containing acid blue 22 by electrochemical oxidation. *Journal of Hazardous Materials*, *153*(1–2), 83–88. https://doi.org/10.1016/j.jhazmat.2007.08.023

Parshetti, G. K., Parshetti, S. G., Telke, A. A., Kalyani, D. C., Doong, R. A., & Govindwar, S. P. (2011). Biodegradation of Crystal Violet by Agrobacterium radiobacter. *Journal of Environmental Sciences*, *23*(8), 1384–1393. https://doi.org/10.1016/S1001-0742(10)60547-5

Parshetti, G., Kalme, S., Saratale, G., & Govindwar, S. (2006). Biodegradation of malachite green by Kocuria rosea MTCC 1532. *Acta Chimica Slovenica*, *53*(4), 492–498.

Pazarlioglu, N. K., Urek, R. O., & Ergun, F. (2005). Biodecolourization of Direct Blue 15 by immobilized Phanerochaete chrysosporium. *Process Biochemistry*, *40*(5), 1923–1929. https://doi.org/10.1016/j.procbio.2004.07.005

Pramanik, S. K., & Rana, M. (2017). *Bioelectricity Generation Using Carbon Felt Electrode in Microbial Fuel Cell ( MFC ) Inoculated With Mixed Cultures Bioelectricity Generation using Carbon Felt Electrode in Microbial Fuel Cell ( MFC ) Inoculated with Mixed Cultures*. *July*. https://doi.org/10.17737/tre.2017.3.2.0039

Rafatullah, M., Sulaiman, O., Hashim, R., & Ahmad, A. (2010). Adsorption of methylene blue on low-cost adsorbents: A review. *Journal of Hazardous Materials*, *177*(1–3), 70–80. https://doi.org/10.1016/j.jhazmat.2009.12.047

Rajkumar, D., Song, B. J., & Kim, J. G. (2007). Electrochemical degradation of Reactive Blue 19 in chloride medium for the treatment of textile dyeing wastewater with identification of intermediate compounds. *Dyes and Pigments*, *72*(1), 1–7. https://doi.org/10.1016/j.dyepig.2005.07.015

Reza, M., Dargahi, A., & Shabanloo, A. (2020). Electrochemical degradation of methylene blue dye using a graphite doped PbO 2 anode : Optimization of operational parameters , degradation pathway and improving the biodegradability of textile wastewater. *Arabian Journal of Chemistry*, *13*(8), 6847–6864. https://doi.org/10.1016/j.arabjc.2020.06.038

Rodríguez-Couto, S., Osma, J. F., & Toca-Herrera, J. L. (2009). Removal of synthetic dyes by an eco-friendly strategy. *Engineering in Life Sciences*, *9*(2), 116–123. https://doi.org/10.1002/elsc.200800088

Rong, F. (2015). *Study of Electrochemical Degradation of Bromophenol Blue at Boron-doped Diamond Electrode by Using Factorial Design Analysis*. *12*, 0–5.

Salleh, M. A. M., Mahmoud, D. K., Karim, W. A. W. A., & Idris, A. (2011). Cationic and anionic dye adsorption by agricultural solid wastes: A comprehensive review. *Desalination*, *280*(1–3), 1–13. https://doi.org/10.1016/j.desal.2011.07.019

Sasidharan Pillai, I. M., & Gupta, A. K. (2016). Electrochemical degradation of malachite green: Multivariate optimization, pathway identification and toxicity analysis. *Journal of Environmental Science and Health - Part A Toxic/Hazardous Substances and Environmental Engineering*, *51*(13), 1091–1099. https://doi.org/10.1080/10934529.2016.1199640

Sekomo, C. B., Rousseau, D. P. L., Saleh, S. A., & Lens, P. N. L. (2012). Heavy metal removal in duckweed and algae ponds as a polishing step for textile wastewater treatment. *Ecological Engineering*, *44*, 102–110. https://doi.org/10.1016/j.ecoleng.2012.03.003

Sharma, K. P., Sharma, S., Sharma, S., Singh, P. K., Kumar, S., Grover, R., & Sharma, P. K. (2007). A comparative study on characterization of textile wastewaters (untreated and treated) toxicity by chemical and biological tests. *Chemosphere*, *69*(1), 48–54. https://doi.org/10.1016/j.chemosphere.2007.04.086

Shewa, W. A., Chaganti, S. R., & Lalman, J. A. (2013). Electricity generation and biofilm formation in microbial fuel cells using plate anodes constructed from various grades of graphite. *Journal of Green Engineering*, *4*(1), 13–32. https://doi.org/10.13052/jge1904-4720.412

Shivangi, R., Richa, S., Subhash, C., & ra. (2013). Microbial degradation of synthetic textile dyes: A cost

effective and eco-friendly approach. *African Journal of Microbiology Research*, *7*(24), 2983–2989. https://doi.org/10.5897/ajmr12.1804

Singh, S., Srivastava, V. C., & Mall, I. D. (2013). Mechanism of dye degradation during electrochemical treatment. *Journal of Physical Chemistry C*, *117*(29), 15229–15240. https://doi.org/10.1021/jp405289f

Solís, M., Solís, A., Pérez, H. I., Manjarrez, N., & Flores, M. (2012). Microbial decolouration of azo dyes: A review. *Process Biochemistry*, *47*(12), 1723–1748. https://doi.org/10.1016/j.procbio.2012.08.014

Sun, J., Bi, Z., Hou, B., Cao, Y. qing, & Hu, Y. you. (2011). Further treatment of decolorization liquid of azo dye coupled with increased power production using microbial fuel cell equipped with an aerobic biocathode. *Water Research*, *45*(1), 283–291. https://doi.org/10.1016/j.watres.2010.07.059

Sun, J., Hu, Y. you, Bi, Z., & Cao, Y. qing. (2009). Simultaneous decolorization of azo dye and bioelectricity generation using a microfiltration membrane air-cathode single-chamber microbial fuel cell. *Bioresource Technology*, *100*(13), 3185–3192. https://doi.org/10.1016/j.biortech.2009.02.002

Sun, J., Li, Y., Hu, Y., Hou, B., Xu, Q., Zhang, Y., & Li, S. (2012). Enlargement of anode for enhanced simultaneous azo dye decolorization and power output in air-cathode microbial fuel cell. *Biotechnology Letters*, *34*(11), 2023–2029. https://doi.org/10.1007/s10529-012-1002-8

Tawfik, A., Zaki, D. F., & Zahran, M. K. (2014). Degradation of reactive dyes wastewater supplemented with cationic polymer (Organo Pol.) in a down flow hanging sponge (DHS) system. *Journal of Industrial and Engineering Chemistry*, *20*(4), 2059–2065. https://doi.org/10.1016/j.jiec.2013.09.031

Tayla, K., Aziz, F., Anna, S., Sumaira, J., Naheed, A., & Sayyada, G. (2016). *++Buscar Thesis Microbial decolorization of textile dye effluent.pdf*.

Taylor, P., Sangeetha, T., & Muthukumar, M. (2014). *Energy Sources , Part A : Recovery , Utilization , and Environmental Effects Catholyte Performance as an Influencing Factor on Electricity Production in a Dual-chambered Microbial Fuel Cell Employing Food Processing Wastewater Catholyte Performance as an*. *October 2014*, 37–41. https://doi.org/10.1080/15567030903397966

*UV-3600i Plus Three-detector UV-Vis-NIR Spectrophotometer*. (n.d.). Retrieved November 17, 2022, from https://www.ssi.shimadzu.com/products/uv-vis/uv-vis-nir-spectroscopy/uv-3600i-plus/index.html

Venkata Mohan, S., Saravanan, R., Raghavulu, S. V., Mohanakrishna, G., & Sarma, P. N. (2008). Bioelectricity production from wastewater treatment in dual chambered microbial fuel cell (MFC) using selectively enriched mixed microflora: Effect of catholyte. *Bioresource Technology*, *99*(3), 596–603. https://doi.org/10.1016/j.biortech.2006.12.026

Verma, P., & Madamwar, D. (2003). Decolourization of synthetic dyes by a newly isolated strain of Serratia marcescens. *World Journal of Microbiology and Biotechnology*, *19*(6), 615–618. https://doi.org/10.1023/A:1025115801331

Wang, C., Wang, F., Xu, M., Zhu, C., Fang, W., & Wei, Y. (2015). Electrocatalytic degradation of methylene blue on Co doped Ti/TiO2 nanotube/PbO2 anodes prepared by pulse electrodeposition. *Journal of Electroanalytical Chemistry*, *759*, 158–166.

https://doi.org/10.1016/j.jelechem.2015.11.009

Yao, Y., Li, M., Yang, Y., Cui, L., & Guo, L. (2019). Electrochemical degradation of insecticide hexazinone with Bi-doped PbO2 electrode: Influencing factors, intermediates and degradation mechanism. *Chemosphere*, *216*, 812–822. https://doi.org/10.1016/j.chemosphere.2018.10.191

Yaseen, D. A., & Scholz, M. (2017). Comparison of experimental ponds for the treatment of dye wastewater under controlled and semi-natural conditions. *Environmental Science and Pollution Research*, *24*(19), 16031–16040. https://doi.org/10.1007/s11356-017-9245-5

Zainal, Z., Lee, C. Y., Hussein, M. Z., Kassim, A., & Yusof, N. A. (2005). Effect of supporting electrolytes in electrochemically-assisted photodegradation of an azo dye. *Journal of Photochemistry and Photobiology A: Chemistry*, *172*(3), 316–321. https://doi.org/10.1016/j.jphotochem.2004.12.021

Zeng, G., Ye, Z., He, Y., Yang, X., Ma, J., Shi, H., & Feng, Z. (2017). Application of dopamine-modified halloysite nanotubes/PVDF blend membranes for direct dyes removal from wastewater. *Chemical Engineering Journal*, *323*, 572–583. https://doi.org/10.1016/j.cej.2017.04.131

Zhang, L., Wei, F., Zhao, Q., Chen, X., & Yao, Y. (2019). *Electrochemical degradation of bromophenol blue on porous -PbO 2 –ZrO 2 composite electrodes*. *0123456789*. https://doi.org/10.1007/s11164-019-04040-7

Zhao, Q., Wei, F., Zhang, L., Yang, Y., Lv, S., & Yao, Y. (2019). Electrochemical oxidation treatment of coal tar wastewater with lead dioxide anodes. *Water Science and Technology*, *80*(5), 836–845. https://doi.org/10.2166/wst.2019.323

Zou, H., & Wang, Y. (2017). Azo dyes wastewater treatment and simultaneous electricity generation in a novel process of electrolysis cell combined with microbial fuel cell. *Bioresource Technology*, *235*, 167–175. https://doi.org/10.1016/j.biortech.2017.03.093

# APPENDICES

**Appendix 1: Microbial degradation flask**

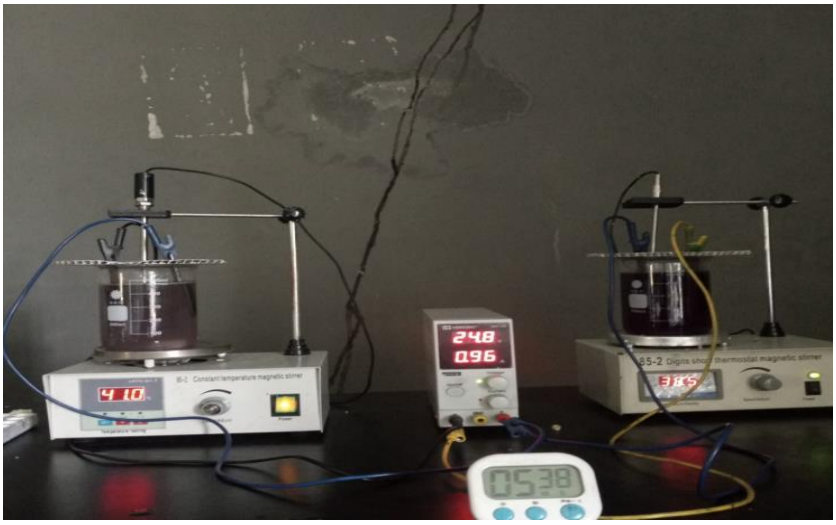


**Appendix 2: Electrochemical degradation setup**

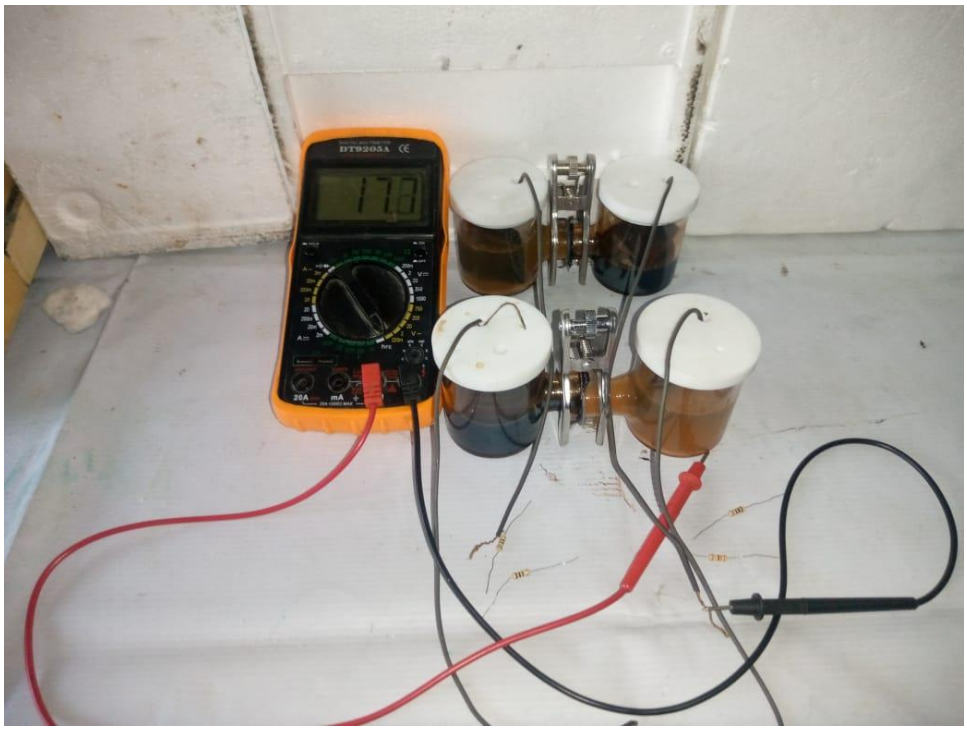


**Appendix 3: Microbial Fuel Cell Setup**